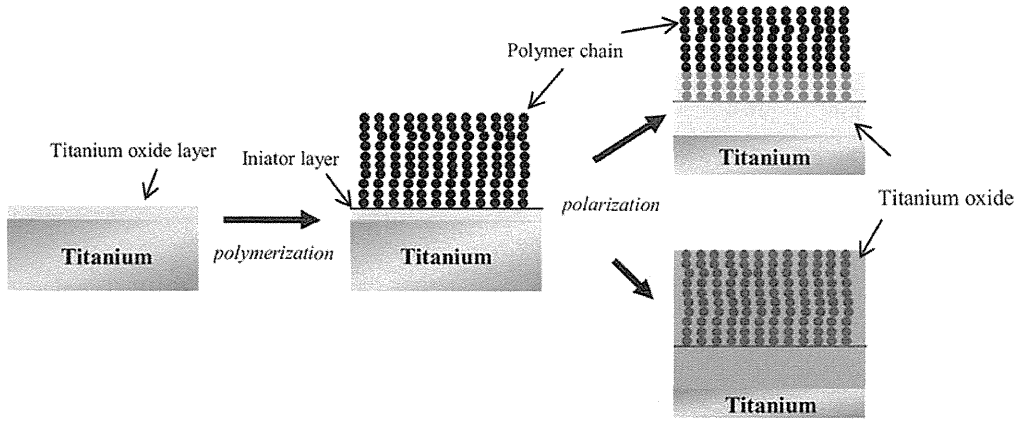

Figure 1. Preparation of polymer brush and polymer–metal oxide nanocomposite.

(30 × 080 mm: bead size = 6 μm, pore size = 20–3000 Å) using refractive index. DMF was used as an eluent with a flow rate of 0·8 ml/min, polyethylene glycol as the standard to calculate the polymer yield and polydispersity index (PDI). The thicknesses of the initiator layer and high density polymer brush grafted on the substrate were measured using an auto ellipsometer with a rotating analyzer (DVA-36L3, Mizojiri Optical Co., Japan). The polarizer angle was 45° and the incident angle was 70°. The calculation of thickness of the brush layer was executed using the mathematical equation (Yoshikawa *et al* 2006):

$$\sigma = L_\rho N_A / M_n, \quad (1)$$

where L is the thickness of graft layer, ρ the bulk density of poly(HEMA) (1·15 g/cm^3), N_A the Avogadro number and M_n the number-average molecular weight.

All the procedures were carried out in an environment where the water and oxygen concentration in air was < 0.1 ppm. The surface of the titanium oxide, polymer brush and nanocomposite was observed with AFM (SPA300, Seiko Instruments Inc., Japan) using a silicon microcantilever (SI-AF01, Seiko Instruments Inc., Japan).

2.2 *Anodic polarization*

Anodic polarization was carried out by using a potentiostat (HA-501G, Hokuto Denko Corp., Japan). A saturated calomel electrode (SCE) and Pt electrode were used as reference and counter electrodes, respectively. The substrate was fixed in a polytetrafluoroethylene holder with an o-ring. The surface area of the substrate in contact with the electrolyte was 0·278 cm^2. Details of the working electrode are described elsewhere (Tanaka *et al* 2007). After immersing the substrate into 0·1 M Na_2SO_4 solution for 10 min, anodic potentials of 10 V_{SCE} were applied for 30 s.

2.3 *Characterization*

In order to observe existence of polymer within the metal oxide, we chose nanocomposite prepared by anodic potentials of 10 V_{SCE}. X-ray photoelectron spectroscopic (XPS) and Auger electron spectroscopic (AES) studies were performed with an electron spectrometer (SSX-100, Surface Science Instruments, USA) and JAMP-7100, JEOL, Japan. All binding energies mentioned in this paper are relative to the Fermi level, and all spectra were excited with a monochromatized AlKα line (1486·61 eV). The photoelectron detector was placed at an angle of 35° with respect to the substrate. The spectrometer was calibrated against the Au $4f_{7/2}$ (binding energy: 84·07 eV) and Au $4f_{5/2}$ (87·74 eV) levels of pure gold and Cu $2p_{3/2}$ (932·53 eV) and Cu $2p_{1/2}$ (952·35 eV) levels and Cu Auger L3M4,5M4,5 line (kinetic energy, 918·65 eV) of pure copper. The energy values were obtained from published data (Asami 1976). In order to estimate the photoelectron peak intensities, the background was subtracted from the measured spectrum according to Shirley's (1972) method.

3. Results and discussion

3.1 *Preparation of polymer brush on titanium substrate*

The composition of the passive titanium oxide surface before grafting the polymer brush was 26·4 mol% of Ti and 73·6 mol% of O. The Ti $2p$ spectrum showed four peaks (Ti^0, Ti^{2+}, Ti^{3+} and Ti^{4+}) and the O $1s$ spectrum showed three peaks (O^{2-}: 56 mol%, OH^-: 29 mol% and H_2O: 11 mol%). The calculated composition of surface of TiO_2 substrate showed a high percentage of TiO_2 and hydroxyl groups. The existence of the hydroxyl group on the surface of the material implies that the ATRP should be initiated by silane coupling. Hence, we

Table 1. Characteristics of poly(HEMA) brush grafted on titanium substrate.

	Thickness[a]	Molecular weight[b]	M_w/M_n	σ[c]	d[d]
Polymer brush	16·4	20,300	1·28	0·56	1·4

[a]Measured by ellipsometry (nm), ± 0·5; [b]measured by GPC (PEG standard); [c]graft density (chain/nm^2). [d]Average distance between nearest grafting points (nm), $d = \sigma^{-1/2}$

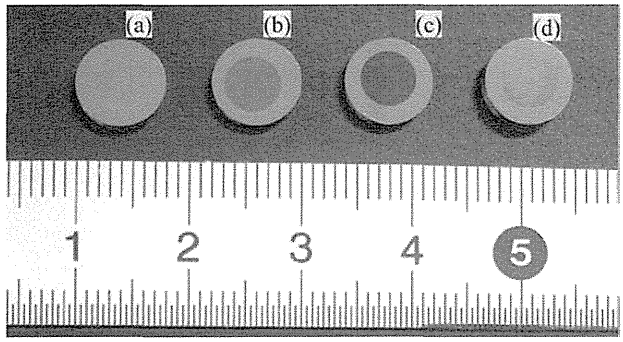

Figure 2. Image of (a) anodic polarized titanium substrate with polymer brush, 0 V_{SCE}, (b) anodic polarized titanium substrate with polymer brush, 3 V_{SCE}, (c) anodic polarized titanium substrate with polymer brush, 10 V_{SCE} and (d) anodic polarized titanium substrate with polymer brush, 30 V_{SCE}.

prepared a polymer brush by a 'surface initiation method' using (2-bromo-2-methyl)propionyloxyhexyltriethoxysilane (BHE) as the initiator (Ohno *et al* 2005; Yoshikawa *et al* 2006, 2010; Nam *et al* 2010). This highly reactive initiator reacts with hydroxyl groups via silane coupling.

Table 1 shows characteristics of the poly(hydroxyethyl methacrylate) (PHEMA) brush grafted on the passive titanium oxide surface. The mechanism of ATRP is simple; Cu(I) complex abstracts the halogen atom of the immobilized initiating dormant species or the grown dormant chain, giving a propagating radical. Then monomer units are added to it until it is recapped to be a dormant chain again. This cycle occurs repeatedly and randomly on the halogenated sites on the surface, which allows all graft chains to grow simultaneously in a controlled fashion (Tsujii *et al* 2006). In our case, density of the polymer brush calculated using (1) was 0·56 chains/nm^2 and its length was ~ 16 nm when Mn was ~ $2{\cdot}0 \times 10^4$. The linear increase in the chain length according to the molecular weight of the poly(HEMA) was confirmed indicating that ATRP was successful (data not shown). According to Tsujii *et al* (2006), the conformation of a polymer brush on a substrate at this graft density is similar to that of a sphere that is randomly and irreversibly adsorbed on a flat surface. According to our calculation, the approximate distance between the polymer chains is 1·4 nm (de Ginnes 1980; Currie *et al* 2003) and the polydispersity index is 1·28, implying that the polymer chain with uniform chain length has been prepared (Yoshikawa *et al* 2006, 2010; Nam *et al* 2010). The unoccupied binding sites of the polymer brush were available for the growth of TiO_2, as shown in figure 1. The polymer brush grafted on the passive titanium oxide surface was stable. Several researchers have reported that Si–O–Ti bonds are unstable; however, we could not find any evidence of the same (Xiao *et al* 1998; Dubrel *et al* 2006). Hence, we concluded that the high density poly(HEMA) brush grafted with on the passive titanium oxide surface with uniform chain length was successfully prepared and was chemically stable.

3.2 *Preparation of polymer–metal oxide nanocomposite*

From table 1, we concluded that the oxidized layer should be controlled to be at least 16 nm to create the hierarchy structure. Furthermore, it is thought that there is enough space for the titanium oxide to grow between the polymer chains, eventually covering the polymer brush layer. However, two questions must be answered in order to prepare a polymer–metal oxide nanocomposite: can anodic polarization occur, regardless of the existence of a dense polymer brush and can the metal oxide mesh be formed in between? Figure 2 shows images of titanium substrate after anodic polarization with the polymer brush. The interference colour of TiO_2 was responsible for the change in colour, and it indicates change in thickness of the oxide layer (van Gils *et al* 2004). We have tested whether the change in colour according to the voltage is the same as bare titanium oxide surface. As shown in figure 3, it can be seen clearly that the change in colour according to the voltage appears from 5 V_{SCE}, where the colour of titanium oxide was light gold. This is because increase in the titanium oxide layer depends on the initial applied voltage. The change of colour was exactly the same from that of bare titanium polarization. This indicates that the growth of TiO_2 was not obstructed by the presence of the dense polymer brush. In other words, oxidation layer grew between the unoccupied binding sites of the polymer brush by electrochemical reaction and chemical reaction, contemporarily. The electrochemical reaction which induces the out-growth of the titanium oxide layer may be suppressed by the polymer chain. This would only induce the chemical reaction, which only makes the oxidization layer thicker inward.

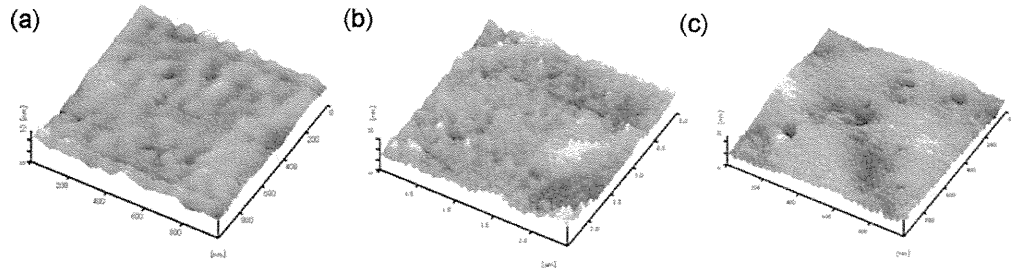

Figure 3. AFM images of (**a**) titanium substrate, (**b**) titanium substrate with polymer brush and (**c**) anodic polarized titanium substrate with polymer brush.

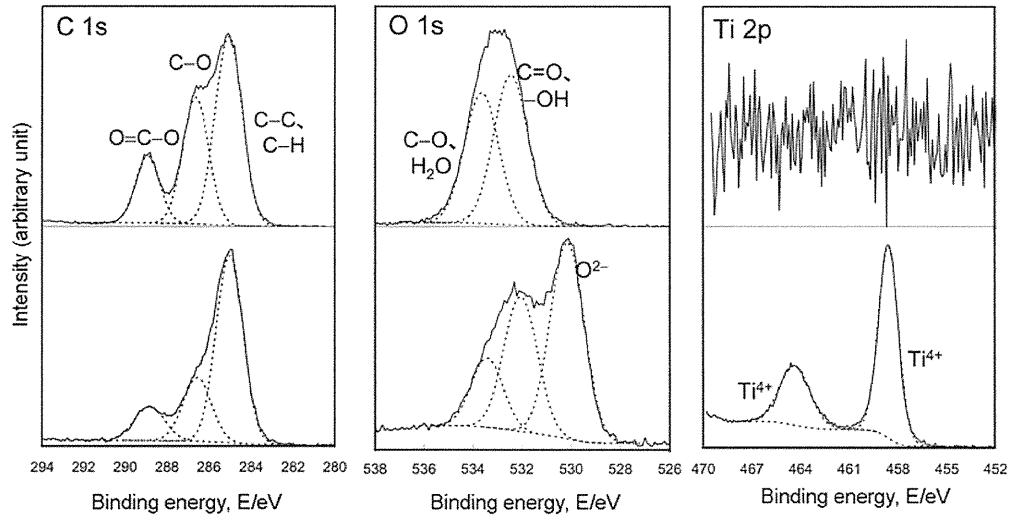

Figure 4. XPS results of titanium oxide with PHEMA brush layer. The upper images are the results of before anodic polarization and below images are the results of after anodic polarization.

3.3 *Surface of polymer–metal oxide nanocomposite*

The surface of the titanium, polymer brush and polarized titanium was observed with atomic force microscope (AFM). An AFM image of the substrate showed that it had a very smooth surface before and after polarization at 10 V_{SCE} (figure 3). The surface of the polymer brush was very smooth because it contained polymer chains that had the same height. The surface after polarization was also very smooth, although it contained few holes. It is thought that the holes are produced by oxygen evolution occurring during the oxidation process. Nonetheless, surface of the titanium oxide layer was smooth and did not show any difference in height by more than 3 nm. This implies that complete anodic polarization was achieved and the polymer chains did not interfere with the polarization process. However, we could not find any specific surface character for 1 or 5 V_{SCE}. Only flat surface was observed which did not provide us any information. So, it was required to confirm that the polymer chain exists after anodic polarization and the titanium oxide layer covers the polymer brush.

3.4 *Confirmation of nanocomposite structure*

To confirm the formation of the polymer–metal oxide composite, XPS and AES measurements were performed. Figure 3 shows XPS spectra for C 1*s*, O 1*s* and Ti 2*p* binding energies from outermost surface area on the nanometric scale (10 V_{SCE}). The presence of a thick and dense PHEMA brush on the titanium substrate before anodic polarization was confirmed (figure 4, upper images), because there was no peak corresponding to TiO_2 in the Ti 2*p* spectrum before the polymer brush was grafted. On the other hand, spectrum of the polarized substrate showed strong peaks in the Ti 2*p* region; Ti^{4+} was determined as the binding state from the binding energy of 458 eV (figure 4, below images). The spectrum of this substrate also showed a new peak due to the O^{2-} binding state at 529 eV in the O 1*s* region. Thus, the

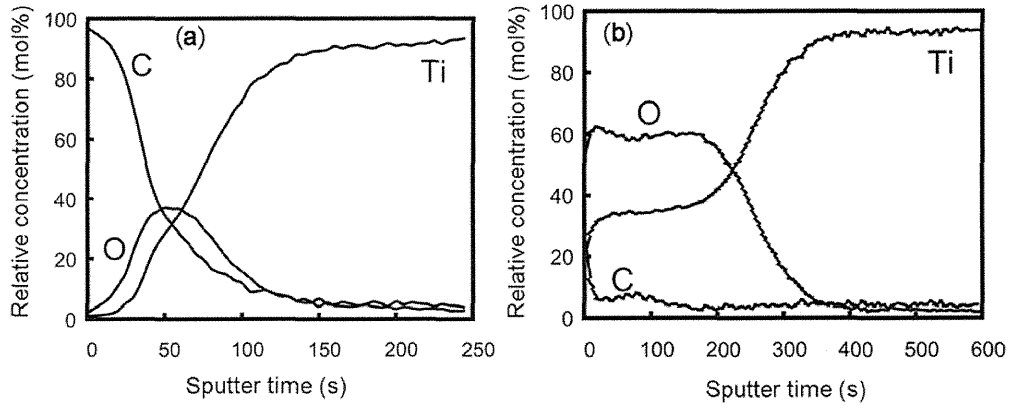

Figure 5. AES results of titanium substrate with PHEMA brush layer (**a**) before and (**b**) after anodic polarization.

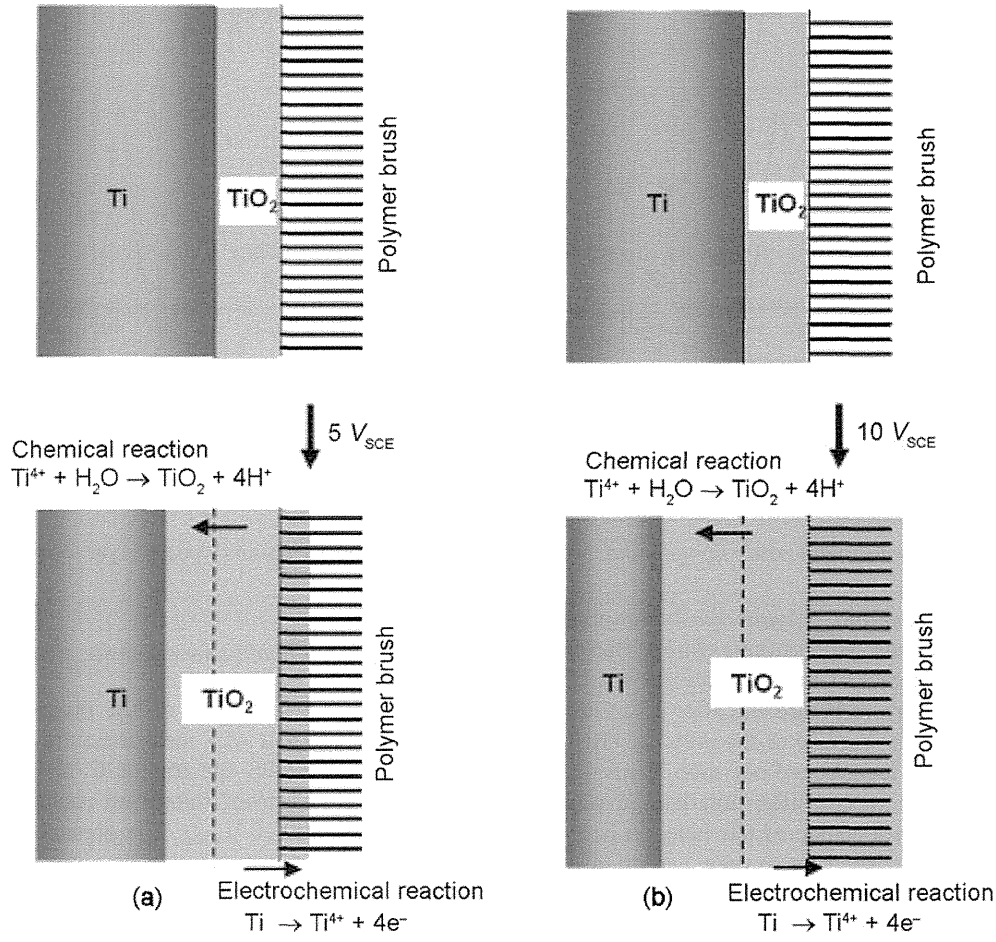

Figure 6. Schematic image of electrochemical and chemical reaction forming titanium oxide layer by anodic polarization via (**a**) 5 V_{SCE} and (**b**) 10 V_{SCE}.

surface of the anodic polarized substrate was almost covered with TiO_2. These results indicate two important facts: the polymer brush is stable on the titanium surface in the aqueous solution and remained stable during the

oxidation process, and the growth of the metal oxide by anodic polarization proceeded, covering the whole polymer brush. On the other hand, XPS result for 5 V_{SCE} was exactly the same as the one with titanium substrate before grafting of the polymer chains (figure not shown), implying that the hierarchy structure of polymer–metal oxide was not formed or has less than 6 nm of the metal oxide formed by electrochemical reaction.

These results were further confirmed by performing an AES measurement for anodic polarization with 10 V_{SCE} (figure 5). An AES depth profile measured before polarization showed three regions: a C-rich layer (PHEMA), an O-rich layer (TiO_2) and a Ti-rich layer (Ti metal). The surface was covered with carbon species, and this result agreed well with the result of XPS characterization. On the other hand, the polarized substrate showed a thick TiO_2 layer. It should be noted that the left half (outer side) of the TiO_2 layer also contained a certain amount of C. The depth of this C–TiO_2 mixed layer was estimated to be about 20 nm with the sputter rate of a SiO_2/Si standard sample, and this value corresponded to the height of the polymer brush. In other words, the upright polymer brush was covered and mixed with the metal oxide by anodic polarization. Hence, AFM result (figure 3) indicates that the polymer brush is located inside the TiO_2 layer and the surface of the nanophase separated polymer–metal oxide nanocomposite is very smooth.

XPS and AES results are direct evidences of the presence of a nanophase separated polymer–metal oxide nanocomposite. However, the hierarchy structure can only be formed when the initial applied voltage is higher than 10 V_{SCE}. That is, the total thickness is required to be at least 30 nm to cover up the polymer brush with the metal oxide layer. Figure 6 shows schematic image of how the titanium oxide is formed according to the different initial applied voltages. The metal oxide layer which covers the polymer brush is electrochemical reaction. From this, it can be postulated that the balance between the in-growing oxidation layer by chemical reaction and out-growing oxidation layer by electrochemical reaction is very important. This is because length of the polymer brush is ~ 16 nm, and at least 16 nm is required to cover the whole polymer brush to from nanophase separated structure (table 1). In the case of low anodic polarization, the electrochemical reaction could not produce enough thickness to cover the polymer chain (figure 6). However, it is impossible to distinguish from the in-growing oxidation layer and out-growing oxidation layer and could not find any proof for this. It can be only assumed that the low initial voltage application have caused thicker formation of the in-growing oxidation layer by chemical reaction. So a comprehensive study on controlling thickness of the metal oxide by electrochemical reaction and chemical reaction is required.

4. Conclusions

We showed that the preparation method used in this study, which is a combination of simple and well known techniques, can be used to successfully produce novel and promising materials. We have obtained three important results. Firstly, contrary to reports on the instability of Si–O–Ti bonds, we found that polymer chains grafted on a TiO_2 surface are stable. Secondly, the application of an appropriate voltage (10 V_{SCE}) to a titanium substrate with a polymer brush leads to the growth of TiO_2 that completely fills up the unoccupied binding sites of the polymer chains, eventually covering the polymer layer with metal oxide. Finally, the polymer need not necessarily be compatible with the metal oxide. The key requirements for polymer-metal oxide nanocomposite preparation are as follows: the surface should have a relevant functional group that can react with the initiator, the polymer brush should be dense and have a homogenous chain length and an appropriate anodic polarization voltage should be applied for the growth of the metal oxide.

We are planning to adjust the thickness of the metal oxide layer to produce a nanoheterogenous surface consisting of organic and inorganic phases. An extensive study on this may lead to the establishment of a preparation method for a new type of surface with a hierarchical structure. Furthermore, it would be possible for us to construct an electrode for biosensor, applying this structure using other metals which is much suitable for electrode.

Acknowledgements

This work was partly supported by Core Research for Evolutional Science and Technology (CREST) of the Japan Science and Technology Agency (JST). The authors would like to acknowledge Prof. Y Tsujii, Kyoto University, Japan, for his advice on ATRP method.

References

Angelomé P C *et al* 2005 *J. Mater. Chem.* **15** 3903
Asami K 1976 *J. Electron Spectrosc.* **9** 469
Beers K *et al* 1999 *Macromolecules* **32** 5772
Currie E P K *et al* 2003 *Adv. Colloid Interf. Sci.* **100–102** 205
de Gennes P G *et al* 1980 *Macromolecules* **13** 1069
Dubruel P *et al* 2006 *Surf. Sci.* **600** 2562
Ivanovici S *et al* 2008 *Macromolecules* **41** 1131
Kickelbick G 2003 *Prog. Polym. Sci.* **28** 83
Lahav M *et al* 2006 *Nano Lett.* **6** 2166
Nam K *et al* 2010 *Chem. Lett.* **39** 1164
Ohno K *et al* 2005 *Macromolecules* **38** 2137
Paul D R and Robeson L M 2008 *Polymer* **49** 3187
Sanchez C *et al* 2001 *Chem. Mater.* **13** 3061

Shirley D A 1972 *Phys. Rev.* **B5** 4709
Sudheendra L and Raju A R 1999 *Bull. Mater. Sci.* **22** 1025
Tanaka Y *et al* 2007 *J. Mater. Sci. Mater. Med.* **18** 797
Tsujii Y *et al* 2006 *Adv. Polym. Sci.* **197** 1
Van Gils S *et al* 2004 *Surf. Coat Technol.* **185** 303
Weatherall I L 1992 *Color Res. Appl.* **17** 352
Wessling B 1997 *Synth. Met.* **85** 1313
Xiao S -J *et al* 1998 *Langmuir* **14** 5507
Xu W *et al* 2008 *Small* **6** 662
Yang Y *et al* 2006 *Polymer* **47** 7374
Yoshikawa C *et al* 2006 *Macromolecules* **39** 2284
Yoshikawa C *et al* 2010 *Chem. Lett.* **39** 142

Langmuir

Article

pubs.acs.org/Langmuir

Wettability and Antifouling Behavior on the Surfaces of Superhydrophilic Polymer Brushes

Motoyasu Kobayashi,*[,†] Yuki Terayama,[‡] Hiroki Yamaguchi,[‡] Masami Terada,[†] Daiki Murakami,[†] Kazuhiko Ishihara,[∥] and Atsushi Takahara*[,†,‡,§]

[†]Japan Science Technology Agency, ERATO, Takahara Soft Interfaces Project

[‡]Graduate School of Engineering and [§]Institute for Materials Chemistry and Engineering, Kyushu University

[∥]Graduate School of Engineering, The University of Tokyo

Supporting Information

ABSTRACT: The surface wettabilities of polymer brushes with hydrophobic and hydrophilic functional groups were discussed on the basis of conventional static and dynamic contact angle measurements of water and hexadecane in air and captive bubble measurements in water. Various types of high-density polymer brushes with nonionic and ionic functional groups were prepared on a silicon wafer by surface-initiated atom-transfer radical polymerization. The surface free energies of the brushes were estimated by Owens-Wendt equation using the contact angles of various probe liquids with different polarities. The decrease in the water contact angle corresponded to the polarity of fluoroalkyl, hydroxy, ethylene oxide, amino, carboxylic acid, ammonium salt, sulfonate, carboxybetaine, sulfobetaine, and phosphobetaine functional groups. The poly(2-perfluorooctylethyl acrylate) brush had a low surface free energy of approximately 8.7 mN/m, but the polyelectrolyte brushes revealed much higher surface free energies of 70−74 mN/m, close to the value for water. Polyelectrolyte brushes repelled both air bubbles and hexadecane in water. Even when the silicone oil was spread on the polyelectrolyte brush surfaces in air, once they were immersed in water, the oil quickly rolled up and detached from the brush surface. The oil detachment behavior observed on the superhydrophilic polyelectrolyte brush in water was explained by the low adhesion force between the brush and the oil, which could contribute to its excellent antifouling and self-cleaning properties.

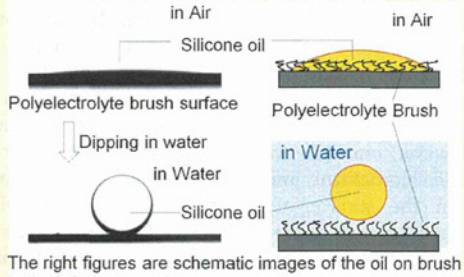

The right figures are schematic images of the oil on brush in the left photographs.

INTRODUCTION

Hydrophilic surfaces and interfaces have attracted much attention because of their applications in water lubrication,[1] antifouling and nonbiofouling surfaces,[2] and biocompatible materials.[3] The surfaces of living cells, cartilage, the vitreous body of eyes, and synovial joints are all hydrophilic surfaces and interfaces consisting of polyelectrolytes that afford excellent biolubrication.[4,5] One of the useful artificial methods of producing a hydrophilic surface is grafting a polymer onto a solid surface. With this method, the wettability and hydrophilicity can be tuned by the chemical structure of the polymer and remain stable for a long period of time because of the covalent anchoring of the polymers to the substrate.

Recently, many types of hydrophilic polymer surfaces with suitable wettability and antifouling properties, especially bioantifouling, have been proposed and prepared by the surface-initiated controlled radical polymerization of vinyl monomers with specially designed hydrophilic functional groups, leading to densely grafted polymers on the solid surface, so-called polymer brushes.[6] For example, the poly(oligoethyleneglycol methacrylate) brush[7] and polysulfobetaine brushes[8,9] have antifouling and nonbiofouling surfaces with good wettability. Théodoly et al. prepared well-anchored polystyrene-*block*-poly(acrylic acid) on a polystyrene film to form a poly(acrylic acid) brush that exhibited wetting transition behavior from partial to total wetting according to deposition conditions.[10] Spruijt et al. achieved surface wettability control of a poly(2-(methacryloyloxy)ethyltrimethylammonium chloride) (PMTAC) brush by changing the counterions and electrode potentials.[11] Superhydrophilic poly[2-(methacryloyloxy)ethyl phosphorylcholine] (PMPC) is well known as an excellent biocompatible and blood-compatible polymer,[12] and its grafted surface shows low friction in aqueous media and humid air.[13,14]

Self-cleaning often depends on the ability of superhydrophobic surfaces to wash out oily contamination particles with water drops flowing on a surface.[15] For example, the leaves of the lotus plant have a typical self-cleaning surface provided by an intrinsic hierarchical structure with randomly oriented hydrophobic wax bosses.[16] Oleophobicity and self-cleaning behavior can also be provided by superhydrophilic surfaces in the wetted state by water.[17−19] For example, fish can maintain a

Received: March 13, 2012
Revised: April 13, 2012
Published: April 16, 2012

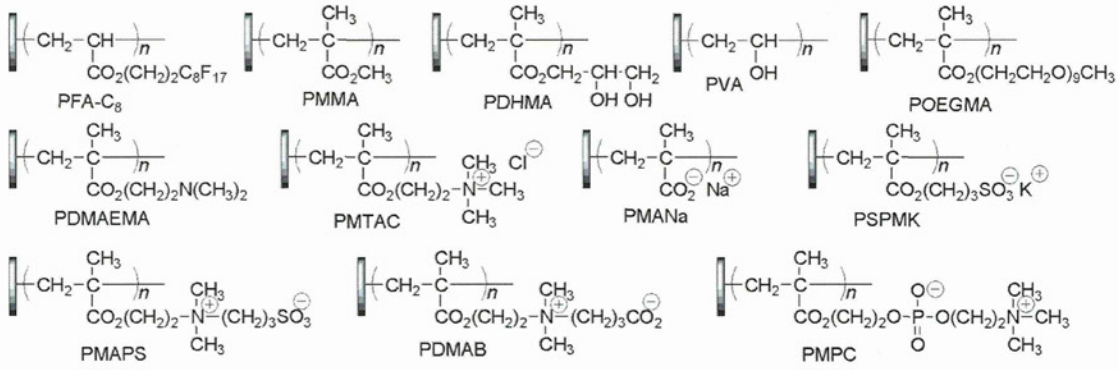

Figure 1. Chemical structures and abbreviations of polymer brushes.

clean body surface even in oil-polluted water. Fish scales are composed of calcium phosphate, protein, and a thin layer of mucus that gives them their hydrophilic behavior, and they are known to be well protected from contamination by oil pollution, marine fouling, and the adhesion of marine organisms. Liu et al. demonstrated that a drop of 1,2-dichloroethane spreads on the surface of fish scales in air. However, once the scales were immersed in water, a drop of 1,2-dichloroethane immediately formed a sphere to flow away from the surface of the fish scales.[20] Hydrophilic nanotechnology in ceramics has already been applied to the development of new dirt- and stain-resistant materials for exterior tiles, which have a surface that absorbs moisture from the air to form a thin water layer.[21] This layer allows dirt adsorbed on the tile surface to be washed off by rainfall. Therefore, it is expected that self-cleaning surfaces can be artificially fabricated by grafting hydrophilic brushes onto substrates.

In this study, both hydrophobic and hydrophilic polymer brushes bearing nonionic and ionic functional groups were prepared by surface-initiated atom-transfer radical polymerization (SI-ATRP) to compare their wettabilities and antifouling properties on the basis of the contact angles of water in air and captive air bubbles as well as hexadecane and silicone oil droplets in water. The oil detachment behavior on swollen hydrophilic brush surfaces in water was explained by the adhesion force between the brush and oil.

In addition, the surface free energies of the brushes were also estimated by different calculation methods, such as Owens' method[22] and the acid–base theory proposed by Fowkes,[23,24] and by van Oss, Chaudhury, and Good.[25] These methods are still being discussed in the field of surface science[26−28] because of the discrepancies in the surface free energy, even that of poly(methyl methacrylate) (PMMA), given by individual methods. However, the surface free energy is scientifically important to an understanding of surface characterization. We tried here to understand the fundamental wettability and antifouling behavior of brush surfaces based on the surface free energy.

EXPERIMENTAL SECTION

Materials. Copper(I) bromide (CuBr, Wako Pure Chemicals) was purified by successive washing with acetic acid and ethanol and was dried under vacuum. Methyl methacrylate (MMA), vinyl acetate (VAc), ethyl iodoisobutylate, and ethyl 2-bromoisobutylate (EB) purchased from Tokyo Chemical Inc. (TCI) were distilled before use. (−)Spartein (Nacalai Tesque) was distilled under reduced pressure and then stored as an anisole solution. Hexadecane (Nacalai Tesque), diiodomethane (Nacalai Tesque), 2,2′-bipyridyl (bpy, Aldrich), 4,4′-dimethyl-2,2′-bipyridyl (Me_2bpy, Aldrich), 4,4′-dinonyl-2,2′-bipyridyl (C_9bpy, Aldrich), 2,2,2-trifluoroethanol (TFE, Acros, 99.9%), and 2,2′-azobis(4-methoxy-2,4-dimethyl valeronitrile) (V-70, Aldrich) were used as received. 2-Perfluorooctylethyl acrylate (FA-C_8) monomer was kindly donated by Daikin Co. Ltd. and was purified by distillation under reduced pressure repeatedly to remove other types of monomer, such as 2-(perfluorodecyl)ethyl acrylate. The purity of FA-C_8 was over 98% by gas chromatography. 2-(*N*,*N*-Dimethylamino)ethyl methacrylate (DMAEMA, TCI) was distilled in the presence of calcium hydride under reduced pressure and was diluted with acetone for storage in a 2.5 M solution. Oligoethylene glycol methacrylate (OEGMA, Aldrich) with nine units of ethylene glycol on the side chain was passed through an aluminum column to remove the stabilizer prior to use. Sulfobetaine-type monomer was freshly synthesized before use by the reaction of DMAEMA and 1,3-puropanesultone and purified by recrystallization in hexane solution to give 3-[dimethyl(2′-methacryloyloxyethyl)ammonio]propanesulfonate (MAPS) as a white powder. MPC monomer was prepared using a previously reported procedure.[12] The other methacrylate monomers, such as methacrylic acid sodium salt (MANa, Wako Chemicals), 3-sulfopropyl methacrylate potassium salt (SPMK, Aldrich), and 4-[dimethyl(2′-methacryloyloxyethyl)ammonio]butanoate (DMAB, Otsuka Chemical Co.), were used as received without any purification. A commercially available MTAC aqueous solution (Aldrich, 80%) was concentrated using a vacuum pump to remove water and then dissolved in TFE. The MTAC/TFE solution was purified by alumina column chromatography and membrane filtration. Deionized water for contact angle measurement was purified with a NanoPure Water system (Millipore Inc.).

Preparation of Polymer Brushes. All brush samples were prepared by the grafting-from method using SI-ATRP from a silicon wafer immobilized with a surface initiator. The surface initiator, (2-bromo-2-methyl)propionyloxyhexyl trimethoxysilane (BHM), was synthesized via the hydrosilylation reaction of 5′-hexenyl (2-bromo-2-methyl)propionate and trimethoxysilane in the presence of Karstedt catalyst[29] and immobilized on a purified silicon wafer by the chemical vapor adsorption method.[30,31] The chemical structures of polymer brushes were illustrated in Figure 1. An unbound initiator as a sacrificial initiator is necessary to control the degree of polymerization and to estimate the number-average molecular weights (M_n) of the resulting polymer.[32] A typical SI-ATRP of MTAC was performed as follows.[33] A few sheets of the BHM-immobilized silicon wafers, 4.0 mL of MTAC/TFE solution (2.0 M), and 0.30 mL of 2-propanol were placed in a well-dried glass tube with a stopcock and then degassed using a freeze−thaw process that was repeated three times. A catalyst solution containing CuBr (0.020 mmol), bpy (0.040 mmol), and EB (0.020 mmol) diluted with TFE was injected into the monomer solution. The resulting reaction mixture was degassed again by repeated freeze−thaw cycles to remove the oxygen and then stirred in an oil bath at 333 K for 16 h under argon, which simultaneously

dx.doi.org/10.1021/la301033h | *Langmuir* 2012, 28, 7212−7222

generated poly(MTAC) brushes from the substrate and free (unbound) poly(MTAC) from EB. The reaction was stopped by opening the glass vessel to air at 293 K. The reaction mixture was poured into THF to precipitate the free polymer and unreacted MTAC. The silicon wafers were washed with methanol using a Soxhlet apparatus for 12 h to remove the free polymer absorbed on their surfaces and dried under nitrogen gas at room temperature.

The PMPC brush was synthesized in a similar manner using CuBr and Me_2bpy in methanol at 303 K for 12 h.[13] SI-ATRP of the FA-C_8 brush was conducted in the presence of CuBr and C_9bpy at 383 K for 72 h under an argon atmosphere to generate the PFA-C_8 brush on the silicon substrate.[34] The PMMA brush was prepared by SI-ATRP using a CuBr/(-)spartein catalyst in anisole at 333 K for 3 days. A poly(2,3-dihydroxypropyl methacrylate) (PDHMA) brush was prepared by SI-ATRP of (2,2-dimethyl-1,3-dioxolan-4-yl)methyl methacrylate (DMM) and successive acid hydrolysis.[35] The PVA brush was prepared by surface-initiated iodide-transfer polymerization of VAc and successive acid hydrolysis.[36] SI-ATRP of OEGMA was performed using CuBr and bpy in methanol at 303 K for 5 days. DMAEMA underwent SI-ATRP by the CuBr/pentamethyldiethyletriamine system in acetone at 303 K for 24 h. SI-ATRP of MAPS was performed in TFE using CuBr and bpy at 303 K for 24 h to give the PMAPS brush.[37] MANa was polymerized in an aqueous solution at pH 8.3 (2.2 M of MANa) using CuBr and Me_2bpy at 298 K for 3 h.[38] SI-ATRP of SPMK was carried out in methanol/water (5/2 v/v, 1.7 M SPMK) at 298 K for 15 h using a reaction system consisting of SPMK/CuBr/$CuBr_2$/Me_2bpy in the following molar ratio: 200/2/0.4/4.[39] The PDMAB brush was prepared by SI-ATRP in the presence of CuBr and bpy in methanol at 333 K for 48 h.

Measurements. The molecular weight and molecular weight distribution of the unbound polymers were estimated by size exclusion chromatography (SEC) using a Shimadzu HPLC system equipped with a multiangle light-scattering detector (MALS, Wyatt Technology DAWN-EOS, 30 mW GaAs linearly polarized laser, wavelength λ = 690 nm) and a refractive index detector (Shimadzu RID-10A, tungsten lamp, wavelength 470–950 nm). The Rayleigh ratio at a scattering angle of 90° was based on that of pure toluene at a wavelength of 632.8 nm at 25 °C. SEC of PMPC was performed with three polystyrene gel columns connected to two super AW3000 and super AW4000 (Tosoh Bioscience) using water containing 0.01 M LiBr as an eluent at a rate of 0.5 mL/min at 313 K. PMAPS required polymethacrylate-based TSKgel columns consisting of G6000PW_{XL}, G5000PW_{XL}, and G3000PW_{XL} (Tosoh Bioscience) using a 200 mM NaCl aqueous solution as an eluent at a rate of 0.8 mL/min at 313 K. In the case of PMTAC, three polystyrene gel columns of Tosho G3000PW_{XL}-CP and two polystyrene gel columns of Tosho G5000PW_{XL}-CP were used with an acetic acid aqueous solution (500 mM) containing sodium nitrate (200 mM) as an eluent at a rate of 0.6 mL/min. SEC of PFA-C_8 was conducted with three gel columns of α6000, α5000, and α4000 (Tosoh Bioscience) using 1,1,1,3,3,3-hexafluoro-2-propanol as an eluent at a rate of 0.5 mL/min. The SEC of PMMA was measured on three gel columns of G5000H_{XL}, G4000H_{XL}, and G3000H_{XL} (Tosoh Bioscience) using THF as an eluent at a flow rate 1.0 mL/min at 313 K. DMF containing 0.01 M LiBr was employed for PDMM, PVAc, PDMAEMA, and POEGMA. Calibration curves were prepared with a series of PMMA standards.

The thickness of the polymer brushes immobilized on a silicon wafer in air (the relative humidity was ca. 45%) was determined by a MASS-102 spectroscopic ellipsometer (Five Lab Co.) with a xenon arc lamp (wavelength 380–890 nm) at a fixed incident angle of 70°. The thickness was also measured by AFM of a partially scratched brush film under vacuum to prevent the influence of moisture. AFM observation was done with E-Seep with an SPI 3800N controller (SII NanoTechnology, Inc.) using a silicon nitride (Si_3N_4) integrated tip on a commercial triangular 200 mm cantilever (Olympus Co., Ltd.) with a spring constant of 0.09 N m^{-1}.

The static and dynamic contact angles were recorded with a DSA10 Mk2 (Krüss, Inc.) drop shape analysis system equipped with a video camera using an inclinable plane. A 2.0 μL droplet of water, diiodomehane, ethylene glycol, formamide, dimethylsulfoxide, or hexadecane was placed on the surface using a micropipet to measure the static contact angle (Figure 2a). The surface free energy and parameters of these probe liquids are listed in Table 1. In an inclinable plane, the sample on the stage was tilted at 2 deg/s until a 30 μL water droplet began to slide down the sample surface. Subsequently, the advancing contact angle (θ_A), the receding contact angle (θ_R), and the sliding angle (θ_S) were determined (Figure 2b).[40] All of these evaluations were conducted in ambient air at room temperature (approximately 298 K). The relative humidity was approximately 40%. The contact angles of a captive air bubble and hexadecane in water were measured on the brush substrate facing downward in a square transparent glass vessel filled with deionized water or hexadecane-saturated water. The air bubble or hexadecane droplet (10 μL) was released from beneath the brush substrate using a microsyringe, as shown in Figure 2c.

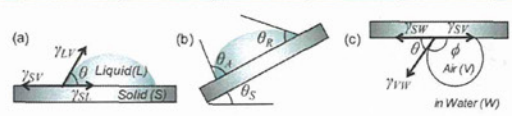

Figure 2. Definitions of static θ, advancing θ_A, receding θ_R, and sliding θ_S contact angles of liquid on a solid surface in air and the contact angle ϕ of an air bubble in water.

RESULTS AND DISCUSSION

Surface Modification by Polymer Brushes. SI-ATRP smoothly proceeded on the BHM-immobilized silicon substrate to give PFA-C_8, PMMA, PDMM, PDMAEMA, PMTAC, and PMPC brushes. The corresponding unbound polymers were also generated from the sacrificial free initiator simultaneously. The M_n values of the unbound polymer brushes were determined with an SEC-MALS system to be 30 000–150 000, which were expected to be the same as those of the corresponding brushes.[33,37,41,42] The thickness of a dried polymer brush film, L, was determined by ellipsometry. Most of the brushes were thicker than 40 nm, except for the PVA brush, which was 20 nm in thickness. The graft density of a brush, σ, was theoretically estimated with the following equation by assuming that the reflective index was uniform in the thin brush layer

$$\sigma = \frac{dL_d N_A \times 10^{-21}}{M_n} \quad (1)$$

where d and N_A are the assumed density of the bulk polymer at 293 K and Avogadro's number, respectively. For example, the σ values of PFA-C_8, PMMA, PDMM, PDMAEMA, and PMPC brushes were 0.15, 0.56, 0.36, 0.40, and 0.23 chains/nm^2, respectively. AFM observation revealed that a homogeneous polymer layer was formed on the substrate and that the surface roughness was 0.8–1.5 nm in a dry state over a 5 × 5 μm^2 scanning area. Hydrolysis of the PDMM brush under mildly acidic conditions produced a PDHMA brush without any elimination of brushes from the substrate.[35] A PVA brush was prepared by the surface-initiated iodide-transfer polymerization of VAc and subsequent acid hydrolysis.[36] Aqueous SI-ATRP of MANa proceeded very quickly in spite of the absence of free initiator and resulted in a polymer brush of 200 nm thickness within a few hours.[38] Similarly, SI-ATRP of SPMK and DMAB were conducted without sacrificial free initiators to result in polyelectrolyte brushes with thicknesses of up to 100 nm.

Table 1. Surface Free Energies and the Acidic and Basic Components of the Liquids Employed[a]

liquid (symbol)[refs]	γ_{LV} (mN/m)	γ_{LV}^{d} (γ_{LV}^{LW}) (mN/m)	γ_{LV}^{p} (γ_{LV}^{AB}) (mN/m)	γ_{LV}^{-} (mN/m)	γ_{LV}^{+} (mN/m)	γ_{LW} (mN/m)
water (W)[44−46]	72.80	21.80	51.00	25.50	25.50	
water (W*)[26]	72.90	22.50	50.40	10.80	58.80	
formamide (F)[43]	58.10	35.50	22.60	11.30	11.30	
formamide (F*)[26]	57.83	32.10	25.73	59.10	2.80	
diiodomethane (I)	50.80	49.50	1.30	0.65	0.65	41.6
diiodomethane (I*)[26]	50.98	50.90	0.08	0.035	0.47	48.5
ethylene glycol (E)[43]	48.00	29.00	19.00	47.00	1.92	
ethylene glycol (E*)[26]	48.10	31.20	16.90	34.00	2.10	
dimethylsulfoxide (D)[43,44]	44.00	36.00	8.00	32.00	0.50	
dimethylsulfoxide (D*)[26]	44.17	34.40	9.77	19.90	1.20	
hexadecane (HD)[44]	27.6	27.6	0.0	0.0	0.0	53.7

[a]The surface free energy of probe liquids (γ_{LV}) and their components attributed to Liftshitz−van der Waals (γ_{LV}^{LW}), the acid−base components (γ_{LV}^{AB}), the electron-donor (γ_{LV}^{-}), and the electron-acceptor (γ_{LV}^{+}) interactions. γ_{LW} is the interfacial free energy of the probe liquid/water.

Table 2. Contact Angle of Various Liquids on the Surfaces of the Polymer Brushes[a]

polymer brushes	water (deg)	diiodomethane (deg)	ethylene glycol (deg)	dimethylsulfoxide (deg)	formamide (deg)	hexadecane (deg)
PFA-C_8	121 ± 0.8	100 ± 0.8	102 ± 0.6	90 ± 1.1	103 ± 1.4	74 ± 1.1
PMMA	74 ± 1.1	36 ± 1.9	49 ± 1.5	22 ± 1.9	60 ± 0.9	<3
PMANa	31 ± 1.4	44 ± 1.4	8 ± 1.1	<3	15 ± 0.8	<3
PMTAC	12 ± 1.3	35 ± 1.5	8 ± 1.9	9 ± 1.8	10 ± 0.9	<3
PSPMK	7 ± 1.6	39 ± 1.1	11 ± 1.7	3 ± 0.5	5 ± 0.9	<3
PMAPS	11 ± 2.1	30 ± 1.8	5 ± 0.8	17 ± 0.9	15 ± 1.3	<3
PMPC	<3	27 ± 1.8	7 ± 1.4	<3	6 ± 1.2	<3

[a]All of the static contact angles were measured with a 2 μL droplet.

Table 3. Contact Angles on Nonionic-Type Polymer Brushes

		PFA-C_8 (deg)	PMMA (deg)	PDHMA (deg)	PVA (deg)	PEGMA (deg)	PDMAEMA (deg)
water	θ: static[a]	121 ± 0.8	74 ± 1.1	60 ± 1.8	45 ± 1.5	44 ± 1.7	56 ± 1.2
	θ_A: advancing[b]	127 ± 0.9	99 ± 1.0	76 ± 2.1	71 ± 0.9	89 ± 0.8[c]	78 ± 1.8
	θ_R: receding[b]	110 ± 1.1	58 ± 0.9	18 ± 1.9	20 ± 0.8	21 ± 0.9[c]	27 ± 1.0
	θ_S: sliding[b]	6 ± 1.2	43 ± 1.7	80 ± 0.6	50 ± 1.2	60 ± 1.5[c]	62 ± 1.3
diiodomethane	θ: static[a]	100 ± 0.8	36 ± 1.9	40 ± 1.8	25 ± 1.1	18 ± 0.9	38 ± 0.9
hexadecane	θ: static[a]	74 ± 1.1	<3	6 ± 0.5	10 ± 0.9	16 ± 1.1	<3
air bubble in water	ϕ: static[d]	59 ± 1.0	104 ± 1.3	145 ± 1.5	142 ± 1.2	142 ± 0.9	138 ± 1.8
hexadecane in water	ϕ: static[d]	<3	89 ± 1.1	108 ± 1.0	119 ± 1.0		

[a]All the static contact angles were measured with a 2 μL droplet. [b]Dynamic contact angles were measured with 30 μL of water. [c]40 μL. [d]ϕ is the supplementary angle for the contact angle of an air bubble (10 μL) in water.

Surface Wettability of Nonionic Polymer Brushes. The water contact angles of polymer brush surfaces are summarized in Tables 2−4. The contact angle measurements were performed at room temperature (298 K) using a contact angle goniometer equipped with video camera recording system operated by software for drop-shape analysis. Three different probe liquids (Milli-Q water, ethylene glycol, and diiodomethane) were used.

Figure 2 illustrates the schematic view of the (a) static and (b) dynamic contact angles of the liquid droplets in air and (c) the contact angle of the air bubble captured on a solid surface in water. The surface free energy γ_{SV} for a solid (S) in contact with saturated vapor (V) is described by the well-known Young equation using the interfacial free energy γ_{SL} at the brush and liquid (L) interfaces

$$\gamma_{SV} = \gamma_{SL} + \gamma_{LV} \cos\theta \quad (2)$$

where γ_{LV} and θ are the surface free energy and the contact angle of the liquid, respectively. When the liquid is water (W), the surface and interfacial free energies are described as γ_{WV} and γ_{SW}. The surface free energy can be described by the extended Fowkes equation using the dispersion force (γ^d) and polar force (γ^p) components.[23]

$$\gamma_{SL} = \gamma_{SV} + \gamma_{LV} - 2(\gamma_{SV}^{d}\gamma_{LV}^{d})^{1/2} - 2(\gamma_{SV}^{p}\gamma_{LV}^{p})^{1/2} \quad (3)$$

where the surface free energy γ_{SV} consists of γ_{SV}^{d} and γ_{SV}^{p}.

$$\gamma_{SV} = \gamma_{SV}^{d} + \gamma_{SV}^{p} \quad (4)$$

Then, eqs 2 and 3 give the Owens-Wendt equation (eq 5):[22]

$$(1 + \cos\theta)\gamma_{LV} = 2(\gamma_{SV}^{d}\gamma_{LV}^{d})^{1/2} + 2(\gamma_{SV}^{p}\gamma_{LV}^{p})^{1/2} \quad (5)$$

Therefore, the surface free energy of the polymer brush can be calculated by the contact angles of two types of liquids with different γ^d and γ^p values, for example, water and diiodomethane, using eq 5. Table 5 displays the interfacial free energies of the polymer brushes versus vapor γ_{SV} and water γ_{SW} evaluated by Owens' method. The γ_{SW} estimated by the water contact angle in the vapor phase is described as γ_{SW}^{V} in Table 5 to distinguish it from γ_{SW}^{W} estimated by the captive bubble

dx.doi.org/10.1021/la301033h | Langmuir 2012, 28, 7212−7222

technique in water, as described later. The surface free energy components of probe liquids attributed to the Liftshitz–van der Waals (γ_{LV}^{LW}) and acid–base components (γ_{LV}^{AB}) and the electron-donor (γ_{LV}^{-}) and electron-acceptor (γ_{LV}^{+}) interactions are listed in Table 1.[43–46]

As shown in Table 3, the PFA-C_8 brush with a broad molecular weight distribution had the highest water contact angle of the brushes, which was 121°, and the lowest surface free energy of 8.6 mN/m for a series of brushes. Typical photographs of water and hexadecane droplets on the surfaces of nonionic-type polymer brushes are displayed in Figure 3.

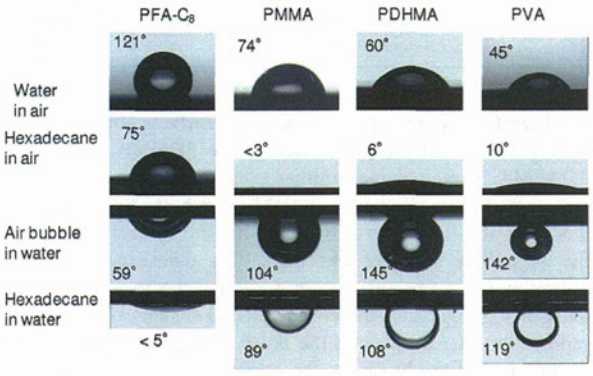

Figure 3. Photographs (side view) of water and hexadecane droplets on polymer brushes in air and an air bubble and hexadecane in contact with the brush surface in water.

The contact angle of hexadecane on the PFA-C_8 brush surface was 74°, implying oleophobic behavior. The low surface tension was caused not only by the low polarity of the C–F bond[47] and the weak molecular interactions of fluorocarbons but also by the unique aggregation structure of perfluorooctyl chains at the brush surface.[48–51] Perfluorooctyl chains at the outermost surface were oriented perpendicular to the substrate surface, forming a densely packed structure to afford a stable hydrophobic surface.[48]

The contact angle of the PFA-C_8 brush surface was influenced by the brush thickness and molecular weight dispersity.[52] When the brush thickness was increased from 4 to 20 nm, the static water contact angle gradually increased from 107 to 120°, which was related to the molecular aggregation state of the perfluoroalkyl (R_f) chains. The orientation of R_f chains at the outermost surface in the PFA-C_8 brush that was thicker than 12 nm was confirmed by a grazing incident wide-angle X-ray diffraction measurement, whereas no diffraction peaks were detected from the thinner PFA-C_8 brush film. The brush that was thicker than 20 nm had an X-ray diffraction pattern caused by the lamellar structure composed of the R_f groups.[34] The densely packed structure of the R_f groups contributed to the reduction in the surface free energy, which was the case for the dependency of the water contact angle on the brush thickness. In this work, a series of polymer brushes with sufficient thickness were prepared to obtain stable contact angles to estimate their surface free energies and specific characteristics.

Polymer brushes with polar functions such as carbonyl, hydroxy, ether, and amino groups had lower water contact angles. PDHMA, PVA, PEGMA, and PDMAEMA are all water-soluble polymers. However, the corresponding polymer brushes had different contact angles depending on their hydrophilicity. Even though hydroxy groups were attached to the side chain or main chain, PDHMA and PVA brushes had relatively high contact angles of 63 and 45°, respectively. Much higher sliding angles and asymmetric drops with high θ_A and low θ_R were observed for PDHMA and PVA brushes than for the other brushes. A water droplet on the PDHMA brush surface did not slide until a tilting angle of 80°, whereas a water droplet on the PMMA brush began to slide when the plate was tilted to 18°.

Generally, contact angle hysteresis on the polymer surface reflects the reorientation of surface polymer chains,[53,54] the rearrangement of the surface structure,[55] topological roughness,[56,57] chemical heterogeneity,[58] and surface defects.[59] When the PDHMA brush was exposed to air (or vapor), the hydrophobic α-methyl group attached to the polymer backbone could be oriented toward the top surface to minimize the interfacial free energy. Alternatively, once the brush was exposed to water, the polar functional groups on the side chain would orient themselves toward the water interface. The strong hydrogen bonding interaction among the hydroxy group and water molecules contributed to a low θ_R, and the α-methyl groups formed a hydrophobic barrier at the air/brush interface, preventing wetting to give a higher θ_A. Large hysteresis and θ_S were also observed for the PEGMA and PDMAEMA brushes. The water contact angle hysteresis is related to the contact angles of air bubbles in water. In addition, the hydrophilic polymer brushes with high graft density were hydrated in water, forming an extended conformation as a result of the osmotic pressure. Therefore, the hydration free energy at the edge of the brush where the water meets the vapor phase should be considered in the study of the water contact angle of a brush,[60,61] as described below.

The contact angles ϕ of the air bubble and hexadecane in water were measured by Hamilton's method (Figure 2c).[62,63] The interfacial energies for brush–water vapor (γ_{SV}), hydrated brush–water (γ_{SW}), and brush–hexadecane (γ_{SO}) were also estimated by Andrade's protocol.[64] Young's equation gives

$$\gamma_{SV} - \gamma_{SW} = \gamma_{WV} \cos\theta \tag{6}$$

where θ is the contact angle of the air bubble filled with water vapor for which Young's equation holds, as shown in Figure 2c. When a drop of hexadecane is in contact with a brush–water interface with an angle of ϕ, the equation should be

$$\gamma_{SW} = \gamma_{SO} + \gamma_{OW} \cos\phi \tag{7}$$

where γ_{OW} is the interfacial energy for hexadecane–water. Hamilton and Andrade et al. assumed the following treatment for the interfacial free energy between hexadecane/solid and solid/water proposed by Fowkes et al.[65] and Tamai et al.[66]

$$\gamma_{SO} \approx \gamma_{SV} + \gamma_{OV} - 2(\gamma_{SV}^{d}\gamma_{OV}^{d})^{1/2} - I_{SO} \tag{8}$$

$$\gamma_{SW} \approx \gamma_{SV} + \gamma_{WV}' - 2(\gamma_{SV}^{d}\gamma_{WV}^{d})^{1/2} - I_{SW} \tag{9}$$

where γ_{WV}' is the surface tension of hexadecane-saturated water and I_{SO} and I_{SW} are polar interaction parameters for the solid/hexadecane and solid/water interfaces, respectively. Parameter I_{SO} is zero because hexadecane is completely nonpolar. γ_{WV}' is approximated to be the same as γ_{WV} because of the extremely low solubility of hexadecane in water. Combining eqs 7–9 gives

$$I_{SW} = \gamma_{WV} - \gamma_{OV} - \gamma_{OW}\cos\phi + 2(\gamma_{SV}^{d}\gamma_{OV}^{d})^{1/2} - 2(\gamma_{SV}^{d}\gamma_{WV}^{d})^{1/2} \tag{10}$$

dx.doi.org/10.1021/la301033h | Langmuir 2012, 28, 7212–7222

Table 4. Contact Angles on Polyelectrolyte Brushes

		PMANa (deg)	PMTAC (deg)	PSPMK (deg)	PDMAB (deg)	PMAPS (deg)	PMPC (deg)
water	θ: static[a]	31 ± 1.4	12 ± 1.3	7 ± 1.6	16 ± 1.4	11 ± 2.1	<3
	θ_A: advancing[b]	66 ± 1.0	50 ± 1.2	32 ± 2.0	18 ± 1.9	24 ± 1.8	13 ± 0.9
	θ_R: receding[b]	13 ± 0.8	12 ± 0.7	3 ± 0.8	6 ± 1.1	<3	<3
	θ_S: sliding[b]	45 ± 1.5	28 ± 2.1	12 ± 1.0	6 ± 2.0	11 ± 2.1	15 ± 1.4
diiodomethane	θ: static[a]	39 ± 1.4	35 ± 1.5	39 ± 1.1	40 ± 1.8	30 ± 1.8	27 ± 1.8
hexadecane	θ: static[a]	<3	<3	<3	<3	12 ± 1.8	<3
ethylene glycol	θ: static[a]	8 ± 1.1	8 ± 1.9	11 ± 1.7	8 ± 1.9	5 ± 0.8	7 ± 1.1
air bubble in water	ϕ: static[d]	154 ± 0.7	156 ± 1.0	160 ± 1.8	148 ± 1.8	155 ± 1.9	170 ± 0.8
hexadecane in water	ϕ: static[d]	170 ± 0.8	151 ± 1.8	176 ± 1.1	158 ± 1.2	175 ± 0.9	175 ± 0.6

[a]All the static contact angles were measured with a 2 μL of droplet. [b]Dynamic contact angles were measured with 30 μL of water. [c]10 μL. [d]ϕ is the supplementary angle for the contact angle of an air bubble (10 μL) in water.

From eq 9, it can be shown that

$$I_{SW} = \gamma_{WV} + (\gamma_{SV} - \gamma_{SW}) - 2(\gamma_{SV}{}^{d}\gamma_{WV}{}^{d})^{1/2} \quad (11)$$

The captive bubble method gives a value of $(\gamma_{SV} - \gamma_{SW})$ from eq 6. Because γ_{WV} = 72.8 mN/m, $\gamma_{WV}{}^{d}$ = 21.8 mN/m, γ_{OV} = $\gamma_{OV}{}^{d}$ = 27.6 mN/m, and γ_{OW} = 53.7 mN/m, I_{SW} and $\gamma_{SV}{}^{d}$ can be calculated by a combination of eqs 10 and 11. $\gamma_{SV}{}^{p}$ can be determined if

$$I_{SW} \approx 2(\gamma_{SV}{}^{p}\gamma_{WV}{}^{p})^{1/2} \quad (12)$$

γ_{SV} was given by $\gamma_{SV}{}^{d}$ and $\gamma_{SV}{}^{p}$ using eq 4. The interfacial energy for the brush–water interface was found with eq 6 and is listed in Table 5 as $\gamma_{SW}{}^{W}$.

Table 5. Surface Free Energy of Polymer Brushes Determined by Owens-Wendt Protocol

polymer brushes	γ_{SV} (mN/m)[a]	γ^{d} (mN/m)	γ^{p} (mN/m)	$\gamma_{SW}{}^{V}$ (mN/m)[b]	$\gamma_{SW}{}^{W}$ (mN/m)[c]
PFA-C_8	8.7	8.4	0.3	46.2	54.8
PMMA	43.8	37.5	6.2	23.7	13.6
PDHMA	48.1	33.0	15.1	11.7	9.3
PVA	59.6	37.5	22.1	8.1	3.8
PEGMA	61.2	39.6	21.6	8.8	
PDMAEMA	50.8	33.4	17.4	10.1	
PMANa	66.6	29.5	37.1	4.3	0.7
PMTAC	72.4	30.5	41.9	0.1	0.1
PSPMK	72.9	28.5	44.4	0.7	0.1
PDMAB	70.8	28.3	42.5	0.8	0.9
PMAPS	73.1	32.5	40.6	1.7	0.7
PMPC	74.5	33.5	41.0	0.2	0.1

[a]Determined with contact angles of water and diiodomethane droplets using parameters W and I in Table 1. [b]The interface energy for brush–water evaluated with the water contact angle in air. [c]The interfacial energy for brush–water evaluated with the captive bubble technique in water.

Photographs of air bubbles and hexadecane droplets attached to the brush surfaces in water are also shown in Figure 3. The contact angle ϕ of the air bubble on the PFA-C_8 brush in water was 59°, which corresponded to the supplementary angle of the water contact angle (θ = 121°) in air to 180°. If there is no surface reorganization, then the sum of ϕ values for the air bubble in water and θ for the water droplet in air should be 180°. The PMMA brush surface, for example, showed θ = 74° for the water contact angle and ϕ = 104° for the air bubble contact angle in water.

However, larger total angles than 180° for the combination of θ and ϕ were observed in the surfaces of nonionic hydrophilic polymer brushes such as the PDHMA, PVA, and PDAEMA. These polymer brushes exhibited large contact angle hysteresis. In the case of the PDHMA brush, the contact angle θ of the water droplet in air was 60° and the contact angle ϕ of the air bubble in water was 145°. This difference might be caused by surface reorganization, including the reorientation of functional groups after the environmental change. Under air or vapor, the water droplet on the brush was pinned at the triple contact line of the brush–water–vapor by the hydrophobic α-methyl groups, preventing wetting and leading to a higher magnitude of θ. In water, the PDHMA brush formed a swollen structure by hydration. When the air bubble was in contact with the hydrated brush surface, a conformational change in the polymer chain occurred to reduce the interfacial free energy between the brush and air. However, it would be hard to exclude the water molecule from the hydrophilic polymer because of the strong hydration force between water and the polar functional groups. A similar situation occurs at the receding water line on the tilted brush substrate in air. As a result, ϕ had a value close to 180° − θ_R, not 180° − θ.

The contact angle of hexadecane in water also depended on the hydrophilicity of the brushes. A hexadecane drop spread on the PFA-C_8 brush surface in water, whereas oleophobicity was observed by the contact angle measurement of hexadecane in air on the PFA-C_8 brush surface.[67] On the contrary, PMMA and PDHMA exhibited a higher contact angle of hexadecane in water in spite of the very low contact angle of hexadecane in air. The hexadecane droplet can easily spread on a hydrophilic surface in air because the surface free energies of hydrophilic brushes γ_{SV} are higher than that of hexadecane γ_{OV} (γ_{LV} = 27.6 mN/m in Table 1). In water, the contact angle of hexadecane is largely governed by γ_{SW} and γ_{OW}, where γ_{OW} is the interfacial energy at the hexadecane–water interface. As listed in Tables 1 and 5, γ_{OW} (γ_{LW} = 53.7 mN/m in Table 1) is significantly larger than γ_{SW} of the hydrophilic brushes to create a self-standing drop shape of hexadecane on the brush surface in water. Parameters $\gamma_{SW}{}^{V}$ and $\gamma_{SW}{}^{W}$ of the hydrophobic PFA-C_8 brush were 46.1 and 54.8 mN/m, respectively, which were close to the value of γ_{OW}. Therefore, a small contact angle of hexadecane in water was observed on the PFA-C_8 brush surface. Conversely, $\gamma_{SW}{}^{W}$ of polar polymer brushes with hydrophilic functional groups were lower than $\gamma_{SW}{}^{V}$, indicating the reduction in the interfacial energy for the brush–water interface in the aqueous environment. The fully hydrated polymer brush in water formed a hydrophilic layer on the

dx.doi.org/10.1021/la301033h | Langmuir 2012, 28, 7212–7222

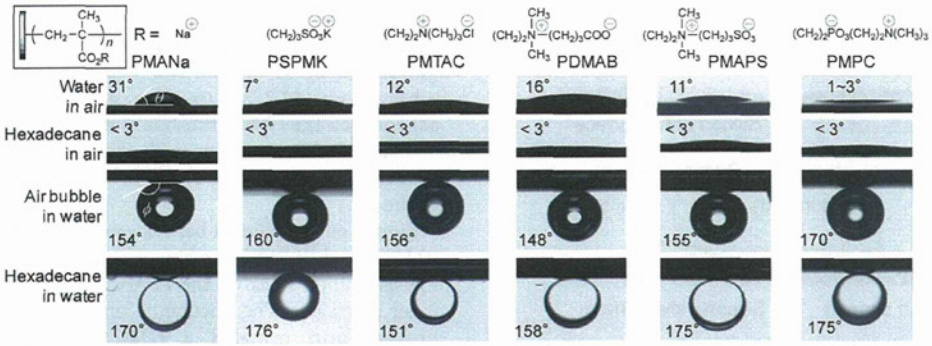

Figure 4. Photographs (side view) of water and hexadecane droplets on polyelectrolyte brushes in air and air bubbles and hexadecane droplets in contact with the brush surfaces in water.

substrate surface, which resulted in antifouling behavior against the hydrocarbon drops.

Surface Wettability of Ionic Polymer Brushes. A water droplet on the polyelectrolyte brush surface had a lower contact angle compared to those of droplets on nonionic-type hydrophilic polymer brushes, as shown in Table 4 and Figure 4. PMANa, PMTAC, PSPMK, PDMAB, and PMPC are water-soluble polymers, whereas PMAPS can be dissolved in an aqueous salt solution. Sulfobetaine groups in PMAPS strongly bind to each other by electrostatic interaction and do not disperse in deionized water at 298 K, resulting in a slightly higher contact angle (11°) for water than for the other zwitterionic-type polyelectrolyte brushes. Although the water contact angle of PMANa was relatively high (31°), the other polyanion, polycation, and zwitterionic-type polyelectrolyte brushes had smaller contact angles. In particular, a very small contact angle of water (3°) was observed on the PMPC brush surface because PMPC adsorbs moisture from the atmosphere like a deliquescent material does.

As shown in Table 5, the surface free energies of polyelectrolyte brushes evaluated by Owens' method were 70–74 mN/m, which were much higher than those of nonionic hydrophilic polymer brushes such as PMMA, PDHMA, and PVA brushes. The surface free energies of the polyelectrolyte brushes were also estimated by the three-liquid acid–base method proposed by van Oss, Chaudhury, and Good (vOCG)[25] in this study. The calculation process of the vOCG method and the surface free energies of polymer brushes are described in the Supporting Information.

When we estimate the surface free energies of the hydrophilic polymer brushes, another important issue to be considered is the partial wetting or total wetting of the hydrophilic polymer brush surface with water. Hydrophilic polymer brushes with a high graft density collapse or shrink in air or in the vapor phase but become hydrated in water to form an extended conformation due to the osmotic pressure. Therefore, the work of hydration at the edge of the brush where the water meets the vapor phase might be considered for the study of the water contact angle of the brush. Cohen Stuart et al. have reported the wetting of PEO brushes.[60] They studied the effect of the bridging of the water/vapor interface by the grafted PEO layer on partial wetting. Théodoly et al. studied the wetting with water of the surface of polystyrene (PS) covered with a poly(acrylic acid) (PAA) brush.[10] They explained how the wetting behavior was governed by the free enthalpy of hydration of the polyelectrolyte monomer units and interfacial tension among PS, PAA, water, and air and the pressure in the brush at the triple contact line of PAA brush–water–vapor. Complete wetting with water can be expected on the surfaces of water-soluble polyelectrolyte brushes such as PMANa and PMPC but might require microscopic observation of the water drop edge as it spreads on the brush surface.

Air Bubble and Oil Detachment from the Polyelectrolyte Brush Surface in Water. Figure 4 displays photographs of air bubbles and hexadecane droplets in water on a series of polyelectrolyte brush surfaces. Most of the air bubbles in contact with the brush surfaces formed spherelike shapes, although some bubbles were deformed by the buoyancy effect. The surfaces of the polyelectrolyte brushes repelled both air bubbles and hexadecane droplets in water. It was difficult to pin an air bubble on the brush surface in water because the bubble was easily swept away by slight vibrations and water flow. When the air bubble in water is released from the lower position and touches the polyelectrolyte brush surface, the air bubble bounces several times. A movie of an air bubble bouncing on the PMPC brush surface in water is available in the Supporting Information. The contact angles of air bubbles and hexadecane in water were observed to remain constant for at least 15–20 min. These results demonstrate the superhydrophilic surfaces prepared with polyelectrolyte brushes.

In air, a hexadecane droplet wets and spreads on the surfaces of polyelectrolyte brushes. However, once the brush substrate was dipped into water, hexadecane detached from the brush surface. Hexadecane and typical hydrocarbon liquids have lower density (0.7–0.8 g/mL) than water. Therefore, they quickly flowed out of the substrate in water. In this work, antifouling behavior in water was observed using silicone oil (Shin-Etsu Chemical Co. KF-96–100CS), the density of which (0.965 g/mL at 293 K) is relatively close to that of water. Figure 5 showed the contact angle of silicone oil on the surface of the PMPC brush and an unmodified silicon wafer in air and in water. The silicone oil immediately spread on the surface of the PMPC brush and the unmodified silicon wafer in air. However, once the brush substrate was dipped into water, the silicone oil quickly formed a sphere that eventually flowed out of the brush surface. The three-phase contact angle θ at the substrate/oil/water interface was 173°. By contrast, the silicone oil remained attached to the unmodified silicon substrate in water (θ = 56°). The movies of silicone oil detachment behavior on PMPC brush surface and nonmodified silicon wafer surface in water are available in the Supporting Information.

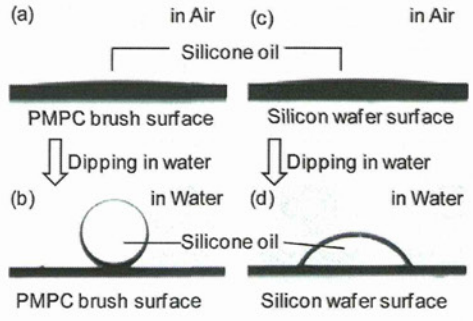

Figure 5. Wettability-reversion phenomena of a silicone oil droplet (5.0 μL, Shin-Etsu Chemical Co. KF-96-100CS) on a PMPC brush (a) in air and (b) in water and on an unmodified silicon wafer (c) in air and (d) in water. Photograph b (side view) displays an oil droplet on a PMPC brush substrate in water, showing the superoleophobicity, with a contact angle of 173°.

The work of adhesion is the amount of reversible work needed to separate a unit area of liquid from the substrate.[68] The work of adhesion in water[69,70] can be expressed as

$$W_{OWS} = \gamma_{SW} + \gamma_{OW} - \gamma_{SO} \quad (13)$$

Combining eqs 13 and 14 (Young's equation) provides a more useful expression for the work of adhesion, as given in eq 15

$$\gamma_{SW} - \gamma_{SO} = \gamma_{OW} \cos\theta \quad (14)$$

$$W_{OWS} = \gamma_{OW}(1 + \cos\theta) \quad (15)$$

Provided both γ_{OW} and θ can be measured experimentally, it is possible to calculate the work of adhesion of oil to the solid under water.[63]

The interfacial free energy (γ_{OW}) of silicone oil/water was estimated to be 7.2 mN/m by the sessile drop method combined with the Young–Laplace equation[71] and the curve-fitting calculation for the drop shape analysis using the density difference between the oil and water ($\Delta\rho$ = density of water (0.997) − density of oil (0.965) = 0.032 g/mL at 293 K). The γ_{OW} value of the silicone oil was much lower than the value of a typical hydrocarbon, such as hexadecane (53.3 mN/m), probably because of some additives in the dimethylsiloxane base oil or polar functional groups attached to the silicone molecules to improve the chemical stability of the product. Using eq 15, the W_{OWS} of silicone oil on the PMPC brush surface was 0.054 mN/m, and W_{ad} of the unmodified silicon substrate was 11.2 mN/m. The small value of the work of adhesion on the PMPC brush in water is assumed to be caused by the excellent affinity with water, which leads to the formation of a water-swollen brush layer and the beading up of the oil.

Similar oil detachment behavior in water was observed on the PMANa and PSPMK brushes, as shown in Figure 6. However, the silicone oil stuck on the PFA-C_8 and PMMA brushes both in air and water. The silicone oil on the PMTAC and PMAPS brushes also revealed a relatively high contact angle (approximately 160°) in water. However, the oil did not flow out from the substrates. In the case of the PMAPS brush, the contact angle of silicone oil increased with the addition of aqueous NaCl solution. When the concentration reached 1.0 M, the contact angle became almost 175°, as shown in Figure 6h, and the silicone oil eventually detached from the PMAPS brush. This oil detachment behavior is closely related to the hydration state of PMAPS. PMAPS is insoluble in deionized water at room temperature but soluble in aqueous salt solution.[72] The chain dimension of PMAPS in aqueous solution increased with the NaCl concentration, which was confirmed by light-scattering measurements and small-angle X-ray scattering.[73,74] Neutron reflectivity measurements revealed that the thickness of swollen PMAPS brushes in aqueous solution increased with the salt concentration from 0 to 1.0 M because the strong attractive dipole–dipole interaction among sulfobetaine units was moderated by the hydrated ions in the aqueous salt solution to induce the switching from a collapsed state to a well-hydrated brush state with a relatively extended chain structure.[75] As a result, the swollen PMAPS brush in aqueous NaCl solution effectively enhanced the oil repellence in aqueous solution. The antifouling effect on a polymer thin film bearing sulfobetaine units was also reported by Gleason.[76] Superhydrophilicity and water promoted the detachment behavior of air bubbles and oils.

The removal of oil drops from solid surfaces immersed in an aqueous medium is of interest in many applications such as self-cleaning, antifogging, and antifouling systems. Oleophobic and antifouling surfaces have been widely fabricated with conventional superhydrophobic materials such as fluoropolymers with micro/nanohierarchical structures like those in a lotus leaf. By

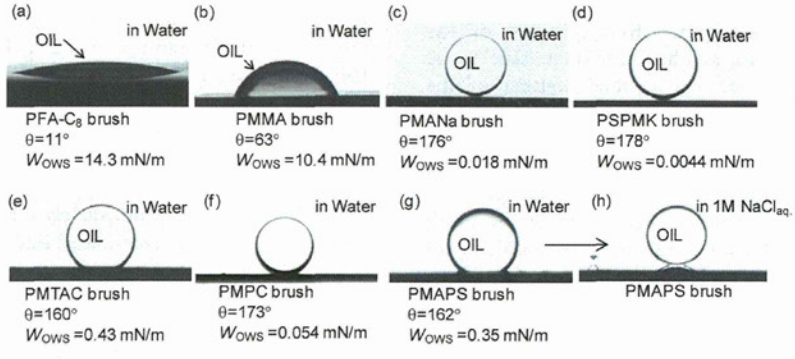

Figure 6. Photographs (side view) of a silicone oil droplet (5.0 μL, Shin-Etsu Chemical Co. KF-96-100CS) on (a) PFA-C_8, (b) PMMA, (c) PMANa, (d) PSPMK, (e) PMTAC, (f) PMPC, and (g) PMAPS brushes in water and (h) the PMAPS brush in a 1.0 M NaCl aqueous solution at 298 K. All of the substrates were immersed in water after the silicone oil was applied in air. The contact angle of the oil droplet in water and the work of adhesion are listed under the photographs.

dx.doi.org/10.1021/la301033h | Langmuir 2012, 28, 7212–7222

contrast, the self-cleaning water/solid interfaces achieved by superhydrophilic polyelectrolyte brush surfaces are proposed here.

■ CONCLUSIONS

Contact angle measurements of water, diiodomethane, hexadecane, and air bubbles were performed to investigate the surface wettabilities of various polymer brushes with hydrophobic perfluoroalkyl and hydrophilic hydroxy groups, amino groups, negatively and positively charged functional groups, and zwitterionic-type electrolyte groups. The fluoropolymer brush had a high water contact angle of up to 121° and a small hysteresis expressed by $\theta_A - \theta_R$, whereas noninoic hydrophilic polymer brushes such as PDHMA, PVA, and POEGMA had relatively small water contact angles and large hystereses. The surface rearrangement of polar functional groups of the polymer brushes might occur as a result of contact with a water droplet in a dry atmosphere. The polyelectrolyte brushes had extremely low water contact angles below 3° and excellent wetting properties with water and hexadecane. The surface free energies of the polyelectrolyte brushes were evaluated to be 70−73 mN/m by Owens' method. Additional theoretical and experimental work is necessary to determine the surface free energy of the polyelectrolyte brushes.

The polyelectrolyte brush surfaces, including PMANa, PSPMK, PMAPS, and PMPC, in aqueous media repelled both air bubbles and hexadecane droplets because of the strong affinity of polyelectrolytes for water. Even when the silicone oil spread on the polyelectrolyte brush surfaces in air, the oil quickly beaded up and detached from the brush surfaces once they were immersed in water. The oil detachment behavior observed on the polyelectrolyte brush in water was explained by the low adhesion force between the hydrate brush and oil, which contributed to excellent antifouling and self-cleaning properties without any surfactants. Thus, one novel strategy for designing a superoleophobic water/solid interface relies on a superhydrophilic surface consisting of ionic polymers, which contrasts with the conventional method using superhydrophobic surfaces. We assume that the fundamental water wettability of various polymer brushes demonstrated in this article is important to the design of surface properties such as friction and adhesion and antifouling properties.

■ ASSOCIATED CONTENT

Ⓢ Supporting Information

Surface free energy components of the PMMA, PFA-C_8, PMANa, PMTAC, PSPMK, PMAPS, and PMPC brush surfaces and the polyelectrolyte brushes calculated by the vOCG protocol. Videos of the oil detachment behaviors and bouncing air bubble on a polyelectrolyte brush in water. This material is available free of charge via the Internet at http://pubs.acs.org.

■ AUTHOR INFORMATION

Corresponding Author

*Motoyasu Kobayashi: Phone, +81-92-802-2543; Fax, +81-92-802-2544; E-mail, motokoba@cstf.kyushu-u.ac.jp. *Atsushi Takahara: Phone, +81-92-802-2517; Fax, +81-92-802-2518; E-mail, takahara@cstf.kyushu-u.ac.jp.

Notes

The authors declare no competing financial interest.

■ ACKNOWLEDGMENTS

We acknowledge Daikin Industries Ltd. for supplying the FA-C_8 monomer.

■ REFERENCES

(1) Klein, J. Shear, friction, and lubrication forces between polymer-bearing surfaces. *Annu. Rev. Mater. Sci.* **1996**, *26*, 581−612.

(2) Xu, F. J.; Neoh, K. G.; Kang, E. T. Bioactive surfaces and biomaterials via atom transfer radical polymerization. *Prog. Polym. Sci.* **2009**, *34*, 719−761.

(3) Tsuruta, T. Contemporary topics in polymeric materials for biomedical applications. *Adv. Polym. Sci.* **1996**, *126*, 1−51.

(4) Lapčík, L., Jr.; Lapčík, L.; De Dmedt, S.; Demeester, J.; Chabrecek, P. Hyaluronan: preparation, structure, properties, applications. *Chem. Rev.* **1998**, *98*, 2663−2684.

(5) Radaeva, F.; Kostina, G. A.; Zmievskii, A. V. Hyaluronic acid: biological role, structure, synthesis, isolation, purification, and applications. *Appl. Biochem. Microbiol.* **1997**, *33*, 111−115.

(6) Rühe, J. Polymer Brushes: On the Way to Tailor-Made Surfaces. In *Polymer Brushes*; Advincula, R. C., Brittain, W. J.; Caster, K. C., Rühe, J., Eds.; Wiley-VCH: Weinheim, Germany, 2004; pp 1−31.

(7) Chen, Y.; Deng, Q.; Xiao, J.; Nie, H.; Wu, L.; Zhou, W.; Huang, B. Controlled grafting from poly(vinylidene fluoride) microfiltration membranes via reverse atom transfer radical polymerization and antifouling properties. *Polymer* **2007**, *48*, 7604−7613.

(8) Chang, Y.; Liao, S.-C.; Higuchi, A.; Ruaan, R.-C.; Chu, C.-W.; Chen, W.-Y. A highly stable nonbiofouling surface with well-packed grafted zwitterionic polysulfobetaine for plasma protein repulsion. *Langmuir* **2008**, *24*, 5453−5458.

(9) Yang, Y.-F.; Li, Y.; Li, Q.-L.; Wan, L.-S.; Xu, Z.-K. Surface hydrophilization of microporous polypropylene membrane by grafting zwitterionic polymer for anti-biofouling. *J. Membr. Sci.* **2010**, *362*, 255−264.

(10) Muller, P.; Sudre, G.; Théodoly, O. Wetting transition on hydrophobic surfaces covered by polyelectrolyte brushes. *Langmuir* **2008**, *24*, 9541−9450.

(11) Spruijt, E.; Choi, E.-Y.; Huck, W. T. S. Reversible electrochemical switching of polyelectrolyte brush surface energy using electroactive counterions. *Langmuir* **2008**, *24*, 11253−11260.

(12) Ishihara, K.; Ueda, T.; Nakabayashi, N. Preparation of phospholipid polymers and their properties as polymer hydrogel membranes. *Polym. J.* **1990**, *22*, 355−360.

(13) Kobayashi, M.; Terayama, Y.; Hosaka, N.; Kaido, M.; Suzuki, A.; Yamada, N.; Torikai, N.; Ishihara, K.; Takahara, A. Friction behavior of high-density poly(2-methacryloyloxyethyl phosphorylcholine) brush in aqueous media. *Soft Matter* **2007**, *3*, 740−746.

(14) Kobayashi, M.; Takahara, A. Tribological properties of hydrophilic polymer brushes under wet conditions. *Chem. Rec.* **2010**, *10*, 208−216.

(15) Nosonovsky, M.; Bhushan, B. Superhydrophobic surfaces and emerging applications: non-adhesion, energy, green engineering. *Curr. Opin. Colloid Interface Sci.* **2009**, *14*, 270−280.

(16) Koch, K.; Bhushan, B.; Barthlott, W. Multifunctional surface structures of plants: an inspiration for biomimetics. *Prog. Mater. Sci.* **2009**, *54*, 137−178.

(17) Marmur, A. Underwater superhydrophobicity: theoretical feasibility. *Langmuir* **2006**, *22*, 1400−1402.

(18) Lord, M. S.; Stenzel, M. H.; Simmons, A.; Milthorpe, B. K. The effect of charged groups on protein interactions with poly(HEMA) hydrogels. *Biomaterials* **2006**, *27*, 567−575.

(19) Genzer, J.; Efimenko, K. Recent developments in superhydrophobic surfaces and their relevance to marine fouling: a review. *Biofouling* **2006**, *22*, 339−360.

(20) Liu, M.; Wang, S.; Wei, Z.; Song, Y.; Jiang, L. Bioinspired design of a superoleophobic and low adhesive water/solid interface. *Adv. Mater.* **2009**, *21*, 665−669.

(21) Matsumoto, H.; Shinkai, S.; Kineshima, K.; Baba, T.; Ohonuki, T.; Kurauchi, H. JP Patent, P2004-99912A.

(22) Owens, D. K.; Wendt, R. C. Estimation of the surface free energy of polymers. *J. Appl. Polym. Sci.* **1969**, *13*, 1741−1747.
(23) Fowkes, F. M. Additivity of intermolecular forces at interfaces. I. Determination of the contribution to surface and interfacial tensions of dispersion forces in various liquid. *J. Phys. Chem.* **1963**, *67*, 2538−2541.
(24) Fowkes, F. M. Quantitative characterization of the acid-base properties of solvents, polymers, and inorganic surfaces. *J. Adhes. Sci. Technol.* **1990**, *4*, 669−691.
(25) van Oss, C. J.; Chaudhury, M. K.; Good, R. J. Interfacial Lifshitz−van der Waals and polar interactions in macroscopic systems. *Chem. Rev.* **1988**, *88*, 927−941.
(26) Della Volpe, C.; Maniglio, D.; Brugnara, M.; Siboni, S.; Morra, M. The solid surface free energy calculation I. In defense of the multicomponent approach. *J. Colloid Interface Sci.* **2004**, *271*, 434−453.
(27) Chibowski, E.; Perea-Carpio, R. Problems of contact angle and solid surface free energy determination. *Adv. Colloid Interface Sci.* **2002**, *98*, 245−264.
(28) Ozcan, C.; Hasirci, N. Evaluation of surface free energy for PMMA films. *J. Appl. Polym. Sci.* **2008**, *108*, 438−446.
(29) Lewis, L. N.; Stein, J.; Smith, K. A.; Messmer, R. P.; Legrand, D. G.; Scott, R. A. In *Progress in Organosilicon Chemistry*; Marciniec, B., Chhojnowski, J., Eds.; Gordon and Breach Publishers: Langhorne, PA, 1993; pp 263−285.
(30) Tada, H.; Nagatama, H. Chemical vapor surface modification of porous glass with fluoroalkyl-functional silanes. 1. Characterization of the molecular layer. *Langmuir* **1994**, *10*, 1472−1476.
(31) Takahara, A.; Hara, Y.; Kojio, K.; Kajiyama, T. Plasma protein adsorption behavior onto the surface of phase-separated organosilane monolayers on the basis of scanning force microscopy. *Colloids Surf., B* **2002**, *23*, 141−152.
(32) Husseman, M.; Malmstrom, E. E.; McNamura, M.; Mate, M.; Mecerreyes, D.; Benoit, D. G.; Hedrick, J. L.; Mansky, P.; Huang, E.; Russell, T. P.; Hawker, C. J. Controlled synthesis of polymer brushes by "living" free radical polymerization techniques. *Macromolecules* **1999**, *32*, 1424−1431.
(33) Kobayashi, M.; Terada, M.; Terayama, Y.; Kikuchi, M.; Takahara, A. Direct synthesis of well-defined poly[{2-(methacryloyloxy)ethyl}trimethyl ammonium chloride] brush via surface-initiated ATRP in fluoroalcohol. *Macromolecules* **2010**, *43*, 8409−8415.
(34) Yamaguchi, H.; Honda, K.; Kobayashi, M.; Morita, M.; Masunaga, H.; Sakata, O.; Sasaki, S.; Takahara, A. Molecular aggregation state of surface-grafted poly{2-(perfluorooctyl)ethyl acrylate} thin film analyzed by grazing incidence X-ray diffraction. *Polym. J.* **2008**, *40*, 854−860.
(35) Kobayashi, M.; Takahara, A. Synthesis and frictional properties of poly(2,3-dihydroxypropyl methacrylate) brush prepared by surface-initiated atom transfer radical polymerization. *Chem. Lett.* **2005**, *34*, 1582−1583.
(36) Terayama, Y.; Kobayashi, M.; Takahara, A. Preparation and surface properties of poly(vinyl alcohol) brush. *Chem. Lett.* **2007**, *36*, 1280−1281.
(37) Terayama, Y.; Kikuchi, M.; Kobayashi, M.; Takahara, A. Well-defined poly(sulfobetaine) brushes prepared by surface-Initiated ATRP using a fluoroalcohol and ionic liquids as the solvents. *Macromolecules* **2011**, *44*, 104−111.
(38) Tugulu, S.; Barbey, R.; Harms, M.; Fricke, M.; Volkmer, D.; Rossi, A.; Klok, H.-A. Synthesis of poly(methacrylic acid) brushes via surface-initiated atom transfer radical polymerization of sodium methacrylate and their use as substrates for the mineralization of calcium carbonate. *Macromolecules* **2007**, *40*, 168−177.
(39) Masci, G.; Bontempo, D.; Tiso, N.; Diociaiuti, M.; Mannina, L.; Capitani, D.; Crescenzi, V. Atom transfer radical polymerization of potassium 3-sulfopropyl methacrylate: direct synthesis of amphiphilic block copolymers with methyl methacrylate. *Macromolecules* **2004**, *37*, 4464−4473.
(40) Extrand, C. W.; Kumagai, Y. An experimental study of contact angle hysteresis. *J. Colloid Interface Sci.* **1997**, *191*, 378−383.
(41) Huang, X.; Wirth, M. J. Surface initiation of living radical polymerization for growth of tethered chains of low polydispersity. *Macromolecules* **1999**, *32*, 1694−1696.
(42) Blomberg, S.; Ostberg, S.; Harth, E.; Bosman, A. W.; van Horn, B.; Hawker, C. J. Production of crosslinked, hollow nanoparticles by surface-initiated living free-radical polymerization. *J. Polym. Sci., Part A: Polym. Chem.* **2002**, *40*, 1309−1320.
(43) van OSS, C. J. Surface Tension Components and Parameters of Liquids and Solids. *Interfacial Forces in Aqueous Media*; Marcel Dekker: New York, 1994; pp 170−185.
(44) van OSS, C. J.; Ju, L.; Chaudhury, M. K.; Good, R. J. Estimation of the polar parameters of the surface tension of liquids by contact angle measurements on gels. *J. Colloid Interface Sci.* **1989**, *128*, 313−319.
(45) Jasper, J. J. The surface tension of pure liquid compound. *J. Phys. Chem. Ref. Data* **1972**, *1*, 841−1009.
(46) van Oss, C. J.; Roberts, M. J.; Good, R. J.; Chaudhury, M. K. Determination of the apolar component of the surface tension of water by contact angle measurements on gels. *Colloids Surf.* **1987**, *23*, 369−373.
(47) Pittman, A. G. In *Fluoropolymers*; Wall, L. A., Ed.; Wiley-Interscience: New York, 1972; pp 419.
(48) Honda, K.; Morita, M.; Otsuka, H.; Takahara, A. Molecular aggregation structure and surface properties of poly(fluoroalkyl acrylate) thin films. *Macromolecules* **2005**, *38*, 5699−5705.
(49) Honda, K.; Yakabe, H.; Koga, T.; Sasaki, S.; Sakata, O.; Otsuka, H.; Takahara, A. Molecular aggregation structure of poly(fluoroalkyl acrylate) thin films evaluated by synchrotron-sourced grazing-incidence X-ray diffraction. *Chem. Lett.* **2005**, *34*, 1024−1025.
(50) Honda, K.; Yamaguchi, H.; Kobayashi, M.; Morita, M.; Takahara, A. Surface molecular aggregation structure and surface physicochemical properties of poly(fluoroalkyl acrylate) thin films. *J. Phys.: Conf. Ser.* **2008**, *100*, 012035.
(51) Honda, K.; Morita, M.; Masunaga, H.; Sasaki, S.; Takata, M.; Takahara, A. Room-temperature nanoimprint lithography for crystalline poly(fluoroalkyl acrylate) thin films. *Soft Matter* **2010**, *6*, 870−875.
(52) Yamaguchi, H.; Kikuchi, M.; Kobayashi, M.; Ogawa, H.; Masunaga, H.; Sakata, O.; Takahara, A. Influence of molecular weight dispersity of poly{2-(perfluorooctyl)ethyl acrylate} brushes on their molecular aggregation states and wetting behavior. *Macromolecules* **2012**, *45*, 1509−1516.
(53) Andrade, J. D.; Ma, S. M.; King, R. N.; Dregonis, D. E. Contact angles at the solid-water interface. *J. Colloid Interface Sci.* **1979**, *72*, 488−494.
(54) Andrade, J. D.; Chen, W. Y. Probing polymer surface and interface dynamics. *Surf. Interface Anal.* **1986**, *8*, 253−256.
(55) Tingey, T. G.; Andrade, J. D. Probing surface micro-heterogeneity of poly(ether urethanes) in an aqueous environment. *Langmuir* **1991**, *7*, 2471−2478.
(56) Busscher, H. J.; Van Pelt, A. W. J.; De Boer, P.; De Jong, H. P.; Arends, J. The effect of surface roughening of polymers on measured contact angles of liquids. *Colloids Surf.* **1984**, *9*, 319−331.
(57) Rangwalla, H.; Schwab, A. D.; Yurdumakan, B.; Yablon, D. G.; Yeganeh, M. S.; Dhinojwala, A. Molecular structure of an alkyl-side-chain polymer-water interface: origins of contact angle hysteresis. *Langmuir* **2004**, *20*, 8625−8633.
(58) Extrand, C. W. Contact angles and hysteresis on surfaces with chemically heterogeneous islands. *Langmuir* **2003**, *19*, 3793−3796.
(59) Wang, L.; Wei, J.; Su, Z. Fabrication of surfaces with extremely high contact angle hysteresis from polyelectrolyte multilayer. *Langmuir* **2011**, *27*, 15299−15304.
(60) Cohen Stuart, M. A.; de Vos, W. M.; Leermakers, G. A. M. Why surfaces modified by flexible polymers often have a finite contact angle for good solvents. *Langmuir* **2006**, *22*, 1722−1728.
(61) Muller, P.; Sudre, G.; Théodoly, O. Wetting transition on hydrophobic surfaces covered by polyelectrolyte brushes. *Langmuir* **2008**, *24*, 9541−9550.
(62) Hamilton, W. C. A technique for the characterization of hydrophilic solid surfaces. *J. Colloid Interface Sci.* **1972**, *40*, 219−222.

(63) Nakamae, K.; Miyata, T.; Ootsuki, N. Evaluation of surface characteristics of polymers in water. Measurement of surface free energy in water. *Makromol. Chem. Rapid Commun.* **1993**, *14*, 413−420.
(64) Andrade, J. D.; King, R. N.; Gregonis, D. E.; Coleman, D. L. Surface characterization of poly(hydroxyethyl methacrylate) and related polymers. I. Contact angle methods in water. *J. Polym. Sci., Polym. Symp.* **1979**, *66*, 313−336.
(65) Fowkes, F. M. Attractive forces at interfaces. *Ind. Eng. Chem.* **1964**, *56*, 40−52.
(66) Tamai, Y.; Makuuchi, K.; Suzuki, M. Experimental analysis of interfacial forces at the plane surface of solids. *J. Phys. Chem.* **1967**, *71*, 4176−4179.
(67) Schmidt, D. L.; Coburn, C. E.; Dekoven, B. M.; Potter, G. E.; Meyers, G. F.; Fischer, D. A. Water-based non-stick hydrophobic coatings. *Nature* **1994**, *368*, 39−41.
(68) Comyn, J. Contact angles and adhesive bondings. *Int. J. Adhes. Adhes.* **1992**, *12*, 145−149.
(69) Clint, J. H.; Wicks, A. C. Adhesion under water: surface energy considerations. *Int. J. Adhes. Adhes.* **2001**, *21*, 267−273.
(70) Clint, J. H. Adhesion and components of solid surface energies. *Curr. Opin. Colloid Interface Sci.* **2001**, *6*, 28−33.
(71) Andreas, J. M.; Hauser, E. A.; Tucker, W. B. Boundary tension by pendant drops. *J. Phys. Chem.* **1938**, *42*, 1001−1019.
(72) Schulz, D. N.; Peiffer, D. G.; Agarwal, P. K.; Larabee, J.; Kaladas, J. J.; Soni, L.; Handwerker, B.; Garner, R. T. Phase behaviour and solution properties of sulphobetaine polymers. *Polymer* **1986**, *27*, 1734−1742.
(73) Kikuchi, M.; Terayama, Y.; Hoshino, T.; Kobayashi, M.; Ogawa, H.; Masunaga, H.; Takahara, A. Static and dynamic scattering from polysulfobetaine immobilized on silica nanoparticle in ionic liquid. *J. Phys.: Conf. Ser.* **2011**, *272*, 012016.
(74) Kikuchi, M.; Terayama, Y.; Ishikawa, T.; Hoshino, T.; Kobayashi, M.; Ogawa, H.; Masunaga, H.; Koike, J.; Horigome, M.; Ishihara, K.; Takahara, A. Chain dimension of polyampholytes in solution and immobilized brush states. *Polym. J.* **2012**, *44*, 121−130.
(75) Terayama, Y.; Arita, H.; Ishikawa, T.; Kikuchi, M.; Mitamura, K.; Kobayashi, M.; Yamada, N. L.; Takahara, A. Chain dimensions in free and immobilized brush states of polysulfobetaine in aqueous solution at various salt concentrations. *J. Phys.: Conf. Ser.* **2011**, *272*, 012010.
(76) Yang, R.; Xu, J.; Ozaydin-Ince, G.; Wong, S. Y.; Gleason, K. K. Surface-tethered zwitterionic ultrathin antifouling coatings on reverse osmosis membranes by initiated chemical vapor deposition. *Chem. Mater.* **2011**, *23*, 1263−1272.

View Article Online / Journal Homepage / Table of Contents for this issue
Dynamic Article Links

Soft Matter

Cite this: *Soft Matter*, 2012, **8**, 5477

www.rsc.org/softmatter

PAPER

Designing dynamic surfaces for regulation of biological responses†

Ji-Hun Seo,[ad] Sachiro Kakinoki,[bd] Yuuki Inoue,[cd] Tetsuji Yamaoka,[bd] Kazuhiko Ishihara[cd] and Nobuhiko Yui*[ad]

Received 12th February 2012, Accepted 5th March 2012
DOI: 10.1039/c2sm25318f

ABA block copolymers composed of highly methylated polyrotaxane and hydrophobic anchoring terminal segments containing 2-methacryloyloxyethyl phosphorylcholine (MPC) and *n*-butyl methacrylate (PMB) (OMe-PRX-PMB) were synthesized as a platform of molecularly dynamic biomaterials. A contact angle measurement indicated that polymer surfaces with higher molecular mobility factors (M_f) estimated from quartz crystal microbalance with dissipation (QCM-D) measurements showed more significant changes in hydrophilicity in response to an environmental change between air and water; the OMe-PRX-PMB surface showed the highest M_f among the prepared polymer surfaces. Fibrinogen adsorption and its conformational analysis estimated by QCM-D and enzyme-linked immunosorbent assay revealed that large amounts of fibrinogen adsorption occurred in a soft manner on the OMe-PRX-PMB surface and that the antibody binding to the C-terminus of the fibrinogen γ chains responsible for platelet adhesion and activation decreased as the M_f value increased. Furthermore, it was found that the OMe-PRX-PMB surface showed low platelet adhesion and high fibroblast adhesion, suggesting that molecular movement on biomaterial surfaces could be one of the key parameters in the regulation of a non-specific biological response.

1. Introduction

When artificial materials are placed in a biological environment, protein–material interaction primarily occurs on the surfaces along with the physicochemical properties of materials.[1–3] The state of adsorbed proteins plays a dominant role in most non-specific biological responses such as foreign body reaction or clot formation.[4] Therefore, the development of anti-fouling materials that are able to prevent non-specific protein interaction has been a critical issue in the field of biomaterials for the last several decades.[5] Although several applications of anti-fouling materials have been reported for the limited number of available biomaterials such as artificial blood vessels, anti-fouling properties also prevent the promotion of tissue regeneration on the materials implanted in a damaged body. Because the extracellular matrix composed of protein molecules is an essential factor for cell adhesion and tissue formation, protein adsorption on the biomaterials is a fundamental requirement.[6] However, non-specifically adsorbed surface proteins also can trigger undesirable biological reactions as mentioned above. This paradoxical problem of protein adsorption has been a fundamental barrier to the development of ideal biomaterials that prohibit non-specific biological reactions as well as promote specific cell adhesion. Because conformational change of adsorbed proteins is the cause of most biological responses on the artificial materials, it is important to regulate protein conformation in the design of ideal biomaterials. A number of variables that have an effect on the conformational change of adsorbed proteins have been reported in the last several decades. These include polarity, charge density, and other geometrical factors such as surface roughness.[7–9] Nowadays, these factors are commonly used to regulate biological responses on artificial materials. However, to the best of our knowledge, there have been no reports on key variables responsible for moderate conformational change that can modulate cell adhesion for tissue regeneration and prevent undesirable foreign body reactions such as blood clotting and inflammatory reaction. Not only dynamic cell membranes but also single protein molecules continuously move on the surface of artificial materials until they determine the thermodynamic standpoint for final conformations.[10] Therefore, even well-defined artificial materials with determined surface properties could not withstand the dynamic responses of the biological environment. We presume that rigid material surfaces with a determined surface nature generate conformational changes in adsorbed proteins, and finally trigger undesirable biological responses. Therefore, in this paper, we present a novel concept, which proposes that dynamic material surfaces that flexibly respond to a dynamic biological environment can possibly overcome the limitations of traditional biomaterials.

[a]*Institute of Biomaterials and Bioengineering, Tokyo Medical and Dental University, Tokyo 101-0062, Japan. E-mail: yui.org@tmd.ac.jp; Fax: +81-3-5280-8027; Tel: +81-3-5280-8020*
[b]*Department of Biomedical Engineering, National Cerebral and Cardiovascular Center Research Institute, Suita, Osaka, 565-8565, Japan*
[c]*Department of Materials Engineering, The University of Tokyo, Tokyo 113-8656, Japan*
[d]*JST-CREST, Tokyo 102-0076, Japan*
† Electronic supplementary information (ESI) available: NMR and AFM images. See DOI: 10.1039/c2sm25318f

Polyrotaxane (PRX) is a representative molecular assembly consisting of a host molecule, *e.g.*, α-cyclodextrin (α-CD), threading a guest molecule, *e.g.*, linear polyethylene glycol (PEG). Because both components are not covalently connected, the threaded α-CD molecules are anticipated to be movable along the PEG backbone. Based on this perspective, we have systematically studied the effect of the molecular mobility of polyrotaxanes on biological interaction with proteins. Throughout these studies, we clarified that CD mobility is influential in enhancing multivalent interaction with receptor proteins in biological ligand-immobilized polyrotaxanes.[11–15] Furthermore, we have demonstrated that cytocleavable polyrotaxanes are very effective in DNA delivery to the nucleus in a target cell.[16–21] As polymeric materials for designing movable surfaces using a polyrotaxane structure, the block copolymer containing the PRX segment was previously synthesized by using an atom transfer radical polymerization method with hydrophobic isobutyl methacrylate.[22] The prepared surface showed high molecular mobility and eliminated adsorption of human plasma fibrinogen by introducing a low degree of methoxy (OMe) groups of α-CD molecules on the PRX segment. In this study, we introduced bio-inert poly((2-methacryloyloxyethyl phosphorylcholine)-co-(*n*-butyl methacrylate)) (PMB) anchoring terminals at both ends of the PRX segment by using the reversible addition-fragmentation chain transfer (RAFT) polymerization method. Furthermore, a higher degree of OMe groups were introduced to each threaded α-CD molecule to modulate the protein interaction on the hydrophilic PRX moiety. The aim of this study is to investigate the dynamic interaction of mobile OMe groups with protein molecules and the associated biological responses including platelet and fibroblast adhesion.

2. Materials and methods

2.1 Materials

A 2-methacryloyloxyethyl phosphorylcholine (MPC) was obtained from NOF Co. (Tokyo, Japan). 4-(Benzodithioyl)-4-cyanopentanoic acid (CTA) was synthesized according to a previously reported method.[23] α-CD, BMA, sodium hydride, iodomethane, α,α′-azobisisobutyronitrile (AIBN), and all the organic solvents were purchased from Tokyo Kasei Co. (Tokyo, Japan) and used as received. PEG (number average molecular weight of 20 kDa) (PEG 20k) was purchased from the Sigma-Aldrich Chemical Co. (St. Louis, MO, USA), and the hydroxyl end groups were converted to amine groups by using a previously reported method.[24]

Goat polyclonal antibody to mouse IgG conjugated with horseradish peroxidase (HRP) and anti-fibrinogen alpha antibody (49D2) were purchased from Abcam Inc. (Cambridge, MA, USA), and anti-fibrinogen gamma antibody (clone2 G2. H9) was purchased from Millipore (Bedford, MA, USA). Human plasma fibrinogen was purchased from Sigma-Aldrich (St. Louis, MO, USA) and other biological reagents were purchased from Gibco Invitrogen Corp. (Grand Island, NY, USA).

Fresh blood was donated by a healthy human volunteer at the National Cerebral and Cardiovascular Center Research Institute. The whole blood was collected with 10 v/v% of 3.8% trisodium citrate solution, and platelet-rich plasma (PRP) was prepared *via* a centrifugation process (200 gravity, 15 min at 25 °C). After this, the PRP was further centrifuged (1500 gravity, 10 min at 25 °C) to obtain platelet-poor plasma (PPP). The number of platelets in the PRP was then adjusted by PPP to 1.0×10^7 mL^{-1}. The use of whole blood and platelets were approved by the Biosafety Committee at National Cerebral and Cardiovascular Center Research Institute.

2.2 Block copolymer synthesis

Synthesis of pseudo-PRX macro CTA. Previously, PEG 20k macro chain transfer agent (CTA) was synthesized as follows: 1 g of PEG 20k bis-amine (0.050 mmol), and 0.018 g of dimethylamino pyridine (0.15 mmol) were dissolved in 5 mL of dichloromethane. To this, 0.14 g of CTA (0.50 mmol) and 0.082 g of water soluble carbodiimide (0.50 mmol) were added and stirred for 12 h at room temperature. Next, some fresh dichloromethane was added and the mixture was re-precipitated in cold diethyl ether. The crude product was then dissolved in water, and the dialysis process was carried out (MWCO 3500) for a day, followed by the lyophilization process.

The obtained PEG macro-CTA (0.35 g) was then mixed with 3.5 g of α-CD in 25 mL of water at room temperature until the light-pink and turbid inclusion complex was formed. The precipitate was then isolated by means of the centrifuge process, and washed again with 25 mL of water, followed by a repeat of the centrifugation process. The precipitate was then freeze-dried to obtain pink-colored inclusion complex of pseudo-PRX macro CTA.

Synthesis of PRX-PMB block copolymer. A 0.600 g of pseudo-PRX macro-CTA was allowed to react with 0.354 g of MPC (1.20 mmol) and 0.633 g of BMA (4.45 mmol) monomer in 7 mL of ethanol–toluene (1 : 1) mixed solvent, by using 0.820 mg of AIBN (5.00 μmol) as an initiator. The heterogeneous solution was bubbled with an Ar atmosphere for 15 min prior to placement in a 60 °C oil bath. After 24 h, 15 mL of fresh mixed solvent was added to the solution and the precipitate was obtained by means of the centrifugation process. The obtained polymer was sequentially washed with ethanol, acetone, dimethyl sulfoxide (DMSO), and acetone to remove residual monomers and α-CD. The final precipitate was then dried at 40 °C *in vacuo* and the polymer was obtained as a white powder. A similar process was carried out to synthesize PMB and PEG-PMB by using CAT or PEG-CTA as a macro CTA.

Methylation of PRX-PMB block copolymer. 200 mg of the synthesized PRX-PMB block copolymer was heterogeneously dissolved in 7 mL of dehydrated DMSO. To this, 0.155 g of sodium hydride (6.3 mmol) was added under an Ar atmosphere and mixed for 30 min at room temperature. Next, 0.102 g of iodomethane (0.719 mmol) was slowly injected to the mixture and stirred for 3 h at room temperature. After the pH was neutralized with 6 N HCl solution, the mixture was transferred to a dialysis tube (MWCO0 : 20000) and the dialysis process was carried out for 3 days. The methylated PRX-PMB (OMe-PRX-PMB) block copolymer was then obtained by means of the lyophilization process.

2.3 Surface characteristics

The synthesized polymer (5 mg) was initially dispensed in 5 mL ethanol. After that, 5 mL of water was added to prepare 0.05 wt % of clear polymer solution. Each polymer solution (30 μL) was then uniformly cast on a Cell Desk™ (Sumitomo Bakelite Co., Japan), and dried in a clean box at room temperature for a day. Each polymer surface was stabilized in water for a day prior to the surface characterization and other biological evaluations.

X-ray photoelectron spectroscopy (XPS) was used to analyze the surface chemical elements by using a magnesium K_α source with a take-off angle of 90° (Kratos/Shimadzu, Kyoto, Japan). The characterized elements were C, N, and P and the binding energies were referenced to the C_{1s} peak at 285.0 eV.

The static water and air bubble contact angles were measured using a goniometer (Kyowa Interface Science Co., Tokyo, Japan). Prior to the measurement, the surface tension of water (72 mN m^{-1}) was confirmed by means of the pendant drop method using a Young–Laplace curve-fitting algorithm. Under dry conditions, 3 μL of water droplets were brought in contact with the polymer surface for 30 s, and the contact angles were measured using photographic images. Under wet conditions, 5 μL of air bubble was brought in contact with the surfaces in water, and the contact angles again were measured using photographic images.

Quartz crystal microbalance with dissipation (QCM-D) monitoring of the polymer surfaces was carried out by using Q-sense E1-HO (Meiwafosis Co., LTD, Tokyo, Japan). The molecular mobility at the hydrated surfaces was estimated as follows: the Au sensor was cleaned by applying an O_2 plasma treatment for 5 min and a sequential washing with acetone and ethanol, and dried with Ar blowing. The sensor was placed in an open-type chamber equipped with the QCM-D apparatus at 25 °C. The resonance frequency at 35 MHz ($f_{gold,\ dry}$) and the dissipation energy ($D_{gold,\ dry}$) was then measured. Subsequently, $f_{gold,\ wet}$ and $D_{gold,\ wet}$ in a hydrated state were measured with the bare gold in contact with pure water. After the water was removed from each polymer solution and dried by using a stream of air, 20 mL of it was dropped on the surface. After the surface was dried, the resonance frequencies ($f_{sample,\ dry}$ and $f_{sample,\ wet}$) and dissipation energies ($D_{sample,\ dry}$ and $D_{sample,\ wet}$) of the coated surface in both the dry and hydrated states were measured using the same procedure as above.[22]

2.4 Evaluation of biological responses to the block copolymer surface

Protein adsorption test. The polymer-cast Cell Desk™ was immersed in a 0.3 mg mL^{-1} of fibrinogen solution or 10% human plasma in phosphate buffered saline (PBS, pH 7.4) for 1 h at 37 °C. Next, the samples were rinsed twice with 500 mL of fresh PBS employing the stirring method (300 rpm for 5 min). The adsorbed protein was detached in sodium dodecyl sulfate (SDS, 1 wt% in water) by sonication for 20 min, and the protein concentration in the SDS solution was determined by means of the micro-BCA™ method.

The state of adsorbed fibrinogen was also analyzed by QCM-D measurements. The Au substrate was cast with each polymer solution, and the energy dissipation factor (D) and frequency (f) were stabilized under a flow of PBS (0.1 mL min^{-1}). Then, a 0.3 mg mL^{-1} fibrinogen solution was flowed for 1 h, and fresh PBS was flowed for another 1 h. Each D and f value was continuously monitored during the whole process of protein adsorption. The amount of adsorbed proteins was calculated by using the simplified Sauerbrey equation with an overtone value of 7 and C = 17.7 ng cm^{-2}, as follows:[25]

$$\Delta m = -C\Delta f/n$$

An enzyme-linked immunosorbent assay (ELISA) was carried out to estimate the conformational change of adsorbed fibrinogen as follows: initially, each polymer surface was brought in contact with whole human plasma for 5 min at 37 °C. After rinsing three times with PBS, each sample was brought in contact with 2 μg mL^{-1} of the primary antibody (anti-fibrinogen alpha or gamma) solution for 1 h at room temperature. After rinsing four times with PBS, samples were allowed to react with 8 μg mL^{-1} of the secondary antibody conjugated with HRP in bovine serum albumin (BSA) pre-treated 24 well plates for 2 h. After rinsing six times with PBS-T, 0.5 mL of solution (mixture of 10 mL guanylic acid buffer (pH 3.3), 0.125 mL of 3,3′,5,5′-tetramethylbenzidine (44 mM), and 0.018 mL of H_2O_2) was added to each sample surface in the BSA pre-treated well. After the reaction was quenched with 2 N of sulfuric acid, the absorbance at 450 nm in each resulting solution was measured by a micro plate reader (Multiskan FC, Thermo Fisher Scientific, St. Herblain, France).

Each polymer surface was brought in contact with 500 μL of PRP in a 24 well plate at 37 °C for 2 h. After rinsing three times with fresh PBS, platelet adhesion was quantitatively analyzed by means of lactate dehydrogenase (LDH) assay, and the morphology of adhering platelets was observed using a fluorescent microscope after dying F-actin with rhodamine conjugated phalloidin.[26]

The cell adhesion test using NIH3T3 mouse fibroblast was performed on each polymer surface. Approximately 1.0 × 10^5 cells in 1.0 mL of minimum essential medium (Invitrogen Corp., Carlsbad, CA, USA) supplemented by 10% fetal bovine serum was incubated on polymer surfaces for 6 h. After rinsing with fresh medium, the surface adhering cells were observed using an optical microscope and the number of adhering cells was counted by a Cell Counting Kit #8 (Dojindo, Tokyo, Japan).

3. Results and discussion

3.1 Preparation of PRX block copolymers

Scheme 1 shows the overall concept of this study in preparing molecularly dynamic surfaces for evaluating biological

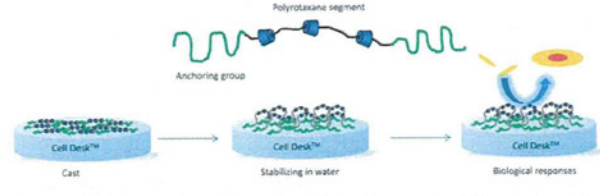

Scheme 1 Schematic explanation of development of dynamic surface.